



**HAL**  
open science

# The influence of restraint on the expansion of concrete due to delayed ettringite formation

Yuichiro Kawabata, Naoshi Ueda, Taito Miura, Stéphane Multon

## ► To cite this version:

Yuichiro Kawabata, Naoshi Ueda, Taito Miura, Stéphane Multon. The influence of restraint on the expansion of concrete due to delayed ettringite formation. *Cement and Concrete Composites*, 2021, 121, pp.104062. 10.1016/j.cemconcomp.2021.104062 . hal-03333586

**HAL Id: hal-03333586**

**<https://hal.insa-toulouse.fr/hal-03333586>**

Submitted on 27 Sep 2023

**HAL** is a multi-disciplinary open access archive for the deposit and dissemination of scientific research documents, whether they are published or not. The documents may come from teaching and research institutions in France or abroad, or from public or private research centers.

L'archive ouverte pluridisciplinaire **HAL**, est destinée au dépôt et à la diffusion de documents scientifiques de niveau recherche, publiés ou non, émanant des établissements d'enseignement et de recherche français ou étrangers, des laboratoires publics ou privés.

1 **The influence of restraint on the expansion of concrete due to delayed ettringite formation**

2

3 **Yuichiro Kawabata<sup>1,\*</sup>, Naoshi Ueda<sup>2</sup>, Taito Miura<sup>3</sup> and Stephane Multon<sup>4</sup>**

4

5 <sup>1</sup> Port and Airport Research Institute, 3-1-1, Yokosuka 239-0826, Japan

6 <sup>2</sup> Department of Civil, Environmental and Applied Systems Engineering, Kansai University, 3-3-35,

7 Yamate-cho, Suita, Osaka, 564-8680, Japan

8 <sup>3</sup> Department of Civil Engineering, Nagoya University, Furo-cho, Chikusa-ku, Nagoya, Aichi, 464-

9 8603, Japan

10 <sup>4</sup> LMDC, Université de Toulouse, INSA/UPS Génie Civil, 135 Avenue de Rangueil, 31077 Toulouse

11 cedex 04, France

12

13 \* Corresponding author: Yuichiro Kawabata

14 Tel.: +81-46-844-5059

15 Fax: +81-46-844-0255

16 Address: 3-1-1, Nagase, Yokosuka 239-0826, Japan

17 E-mail: kawabata-y@p.mpat.go.jp

18

19

20 **Abstract**

21 The influence of restraint on expansion, expansive pressure, and cracking patterns due to delayed  
22 ettringite formation (DEF) in concrete was experimentally evaluated. Especially, the expansive  
23 pressure was estimated with two approaches: calculation from the strain of the steel and direct  
24 measurement using load cells. The expansive behaviors were strongly affected by the restraint,  
25 especially in the restraint direction. The expansive pressure measured by the load cell was 1.9–3.9  
26 MPa, which is nearly consistent with those calculated from the steel bar strain. The expansive pressure  
27 of DEF was almost the same order of magnitude as for ASR expansion, despite larger free DEF  
28 expansion than ASR. From a simplified calculation, it is estimated that the imposed DEF expansion  
29 was reduced from the stress-free expansion by approximately 80%. Although the total length of surface  
30 cracking was independent of the degree of the restraint, the distribution of surface cracks was  
31 significantly modified by the degree of the restraint. On the contrary, the inner crack pattern was  
32 similar for the restraint case while large gap formation was observed for the stress-free case.

33

## 34 **1. Introduction**

35 Delayed ettringite formation (DEF) is a concrete pathology that shows deleterious expansion of the  
36 order of several percent or more in the laboratory, leading to the cracking of concrete and causing  
37 crucial concern in the unexpected deformation or decrease in the integrity of the structures. As an  
38 alkali-silica reaction (ASR), DEF is recognized as an internal swelling reaction in concrete. DEF  
39 expansion is usually more serious than ASR expansion when considering the magnitude of expansion.  
40 While significant effort has been carried out to elucidate the microscope mechanism for DEF  
41 expansion (e.g., [1–3]), fewer studies on structural models are available [4–6]. To assess the  
42 performance of structures affected by DEF, it is important to understand the effect of stress on DEF  
43 expansion. In particular, the extent of the expansive pressure of DEF on concrete and how much stress  
44 is necessary to prevent DEF expansion. While there are fewer studies on such topics, the effect of  
45 restraint on DEF expansion is known to have critical differences from ASR expansion [7–8].

46 At the stress-free condition, DEF expansion can be considered as isotropic whereas ASR  
47 shows intrinsic anisotropy, which may be possibly due to the casting direction [9]. In the case of ASR  
48 under stress, the presence of steel reinforcement as well as active stresses such as prestressing reduces  
49 expansion in the restrained and loading directions [10–22]. According to Multon and Toutlemonde  
50 [13], the expansion is transferred to the direction with lesser compression, resulting in nearly equal  
51 volumetric expansion. Although it remains controversial whether such transfer is always observed for  
52 every concrete (e.g. [14]), “expansion transfer” is one of the key features of ASR expansion under  
53 stress. In contrast, for DEF mortar/concrete, while the expansion in the restrained or loading direction  
54 is reduced, the expansion in the transverse direction without any restraint is almost equivalent to free  
55 expansion [7–8], suggestive of a lack of expansion transfer. This leads to a reduction in the volumetric  
56 expansion of concrete for uni-axially restrained mortar/concrete (20–33% [7–8]). In particular, when  
57 concrete is triaxially reinforced, volumetric expansion is drastically reduced to 54% of that of free  
58 expansion [8].

59 While several studies on expansive pressure of ASR mortar/concrete have been reported [15–  
60 16, 23–26], to the knowledge of the authors, no studies on measuring expansion stress directly have  
61 been reported for the expansive pressure of DEF concrete. For ASR concrete, the expansive pressure  
62 of concrete due to ASR is significantly influenced by many factors, such as the reactivity of the  
63 aggregate and the total alkali content, and ranges from 0.1 to 6 MPa [15–16, 23]. The experimental  
64 conditions of three studies on expansive pressure are summarized in Table 1: two DEF experiments  
65 and one experiment on external sulfate attack (ESA) [27]. Bouzabata et al. [7] considered mortar bar  
66 restrained by four threaded stainless steel bars with different diameters corresponding to reinforcement  
67 ratios ( $A_s/A_c$ ) of 0.8% and 4.9%. Based on the concrete strain at unloading, these investigators reported  
68 compressive stresses at the final expansion of 1.6 and 4.2 MPa for 0.8% and 4.9%  $A_s/A_c$ , respectively.  
69 By applying 14.5 MPa of compressive stress on the DEF concrete, Thiebaut et al. found that creep  
70 exceeds DEF expansion, leading to contraction of the concrete in the longitudinal direction [8]. Similar  
71 to DEF expansion, the expansive pressure of mortar due to ettringite formation subjected to ESA was  
72 measured by Müllauer et al. Thin-walled mortar cylinders were restrained by an inner stainless steel  
73 tension bar and the end-plate disk, and were exposed to sodium sulfate solutions [27]. The resulting  
74 expansive pressure reached around 8 MPa, which is significantly higher than the tensile strength of  
75 mortar.

76 In terms of cracking, both surface and internal cracking must be considered, with the cracking  
77 reducing the mechanical properties of the concrete. For surface cracking, DEF concrete subjected to  
78 uni-axial restraint exhibits oriented cracking along the direction of the restraint, while map cracking is  
79 observed for stress-free DEF concrete [8]. This tendency is similar to ASR, where uni-axial stress  
80 modifies the orientation of the micro-cracks, which may cause an anisotropic modification of the  
81 mechanical properties [14, 22, 28]. At the microstructural scale, when DEF expansion occurs without  
82 external stress, cracks are formed in the cement paste and around aggregates. However, it is unknown  
83 whether the orientation of gaps or microcracks can be modified for DEF under stress.

84           Consequently, there have been fewer studies on structural/mechanical models of concrete  
85 affected by DEF expansion than studies on ASR. In particular, understanding effect of varying degrees  
86 of restraint on DEF expansion and damage (i.e., cracking patterns) is important for assessing the  
87 structural behavior of reinforced concrete. In the present study, experiments with different degrees of  
88 restraint are carried out to evaluate the expansive pressure of concrete due to DEF expansion, with two  
89 approaches adopted: calculation from the strain of the steel and direct measurement using load cells.  
90 The expansive pressures from these approaches are compared in addition to the cracking patterns of  
91 concrete with varying degrees of restraint, which is important for assessing the mechanical response  
92 of concrete damaged by DEF.

93

## 94 **2. Experiments**

### 95 **2.1 Test specimens**

96           Three concrete specimens per case, restrained by steel round bars with different diameters  
97 (9.2, 13, 17, and 26 mm in diameter) were prepared. For one of the three specimens for each case, a  
98 load cell was installed to measure the expansive pressure of the concrete. Hereafter, specimens and  
99 their corresponding case are denoted by the diameter of the steel bar, e.g., “ $\phi$  9.2”. The preparation of  
100 the test specimen is described in the following.

101           The mixture proportion of the concrete is provided in Table 2. The chemical composition of  
102 the high-early-strength Portland cement (Type III Portland Cement) used is shown in Table 3. The  
103 mineral composition by Bogue equation is shown in Table 4. A portion of the cement was replaced by  
104  $K_2SO_4$  reagent so that the total  $SO_3$  content was increased to 5.6% of the cement by weight, with the  
105  $K_2SO_4$  reagent added to the mixing water in advance. Non-reactive sand and gravel were used for  
106 aggregate. The water-to-cement ratio (including  $K_2SO_4$ ) was 0.49.

107           The apparatus for the test including a concrete specimen is shown in Figure 1. The specimens  
108 were cast in a 100×100×340 mm prismatic mold, which had a PVC pipe with an outer and inner

109 diameter of 38 and 32 mm, respectively, placed at the center. Early-age curing was started four hours  
110 after the initiation of the mixing step, following a curing cycle of heating to 90 °C at a rate of  
111 +46.7 °C/h, maintaining for 12 h, and then cooling to 20 °C at a rate of -7 °C/h. Following early-age  
112 curing, the concrete specimens were demolded and the PVC pipe removed. The concrete specimens  
113 were wrapped with plastic film at 20 °C and cured until 28 days. Thereafter, 30-mm thick steel plates  
114 with a 38-mm diameter at their center were placed at the longitudinal ends of the concrete specimens.  
115 In these plates, a small hole was provided to allow the cable of the strain gauge to drain. Additional 6-  
116 mm thick steel plates were added, and a hole in these plates was made to match the diameter of the  
117 steel bar. For a single specimen for each case, a load cell (maximum capacity of 300 kN) was installed  
118 to measure the expansive pressure. A steel bar was inserted through the hole of the specimen and a  
119 small pressure (around 0.1 MPa) applied by tightening the nuts so that the concrete specimen, the steel  
120 bar, and the steel plates were fixed. Two strain gauges (gauge length of 2 mm) were attached to the  
121 surface of the steel bars to monitor their strain. Furthermore, no grouting was applied in the hole so  
122 that no bond stress developed between the concrete and the steel bar. As a typical example, the case  
123 with a 17-mm diameter steel bar is shown in Figure 1. For comparison, a 100×100×400 mm prismatic  
124 specimen without the hole was prepared for stress-free expansion.

125           The compressive strength and Young's modulus for a cylindrical concrete specimen with a  
126 diameter of 100 mm and a length of 200 mm was 32.3 MPa and 28.6 GPa, respectively, before the test  
127 (28 days). After the test, when the expansion was 2.17%, the strength and modulus had decreased to  
128 6.8 MPa and 1.2 GPa, respectively.

129

## 130 **2.2 Expansion test**

131 After assembling the restraint apparatus with the concrete specimens at 28 days, the specimens were  
132 immersed in water. To prevent corrosion of the steel plates and steel bars, they were connected with

133 magnesium alloy as a sacrificial anode. The water was replaced for each measurement. The test  
134 continued until 181 days after the test initiation, when the free expansion had almost reached a plateau.

135 The concrete expansion was measured on the surface of the concrete. The locations of the  
136 measurement points are shown in Figure 2. The concrete specimens were supported on the L-shaped  
137 stainless steel plates and the span was 250 mm during storage and measurement. In Figure 2, the green  
138 points indicate the location of the studs for measuring the longitudinal expansion while the blue points  
139 are similarly the locations for the lateral expansion. The change in the length of the concrete specimens  
140 was measured using a dial gauge for the longitudinal direction and a micrometer for the lateral direction,  
141 each with precisions of 0.001 mm. The expansion was then calculated by dividing the change in length  
142 by the gauge length. The initial length was measured before the test (28 days). The longitudinal  
143 expansion was monitored from the beginning of the test, and measurements of the lateral expansion  
144 began after longitudinal expansion began (70 days after the beginning of the test). The measurement  
145 length of the longitudinal and lateral expansion was 300 and 100 mm, respectively. Measurements  
146 taken at two and three locations for longitudinal and lateral expansion, respectively, for each test  
147 specimen. Strains of the steel bar and expansive pressure were monitored with a data logger. The strain  
148 and pressure were zeroed after specimen insertion in the container filled with water.

149

### 150 **2.3 Crack observation**

151 Surface cracking was observed after 181 days. Cracks were traced by illustration software and the  
152 raster data was converted to vector data. The length and the orientation of the surface cracks were then  
153 analyzed.

154 Afterward, one of the three concrete specimens was cut at the center in the longitudinal  
155 direction, and then half of the specimen was cut longitudinally (100×170 mm). The other half of the  
156 specimen was cut at a thickness of 30 mm perpendicular to the longitudinal direction.



157 The cut samples were impregnated under vacuum with low viscosity fluorescent epoxy resin  
158 with a small amount of ethanol to reduce the viscosity. Subsequently, after releasing the vacuum, 0.3  
159 MPa additional atmospheric pressure was applied to the sample for thirty minutes. After the resin had  
160 hardened sufficiently, the surface of the concrete was roughly ground. Finally, the surface of the  
161 concrete was observed under ultraviolet light. Note that these conventional processes might induce  
162 microcracks or small damage to the specimens whilst comparison between the cases can be possible.  
163

### 164 **3. Results**

#### 165 **3.1 Expansion measured from the concrete surface**

##### 166 **(1) Stress-free expansion**

167 The expansions of the concrete specimens due to DEF in the longitudinal and transverse directions are  
168 illustrated in Figure 3, with the error bars denoting the standard deviations of the measured expansions.  
169 In Figure 3(a), in the stress-free condition, the onset of expansion was around 50 days and exceeded  
170 1.5% at 97 days. The rate of expansion in this interval was around 0.025% per day. Above an expansion  
171 of 1.5%, the rate of expansion gradually reduced with an expansion of 2.0% reached at 139 days, with  
172 a rate of expansion of approximately 0.01%/day. After this time, the expansion begins to plateau.  
173 Similar tendencies can be seen for the cylindrical specimen, although its rate of expansion was slightly  
174 higher. The transverse stress-free expansion, shown in Figure 3(b), was nearly equal to the longitudinal  
175 expansion. The standard deviation of the longitudinal expansion for the prismatic specimen was  
176 smaller than the transverse expansion. This is due to the different gauge lengths, the gauge for the  
177 longitudinal direction being three times longer. Indeed, the longitudinal expansion of the cylindrical  
178 specimen (gauge length of 100 mm) demonstrated a relatively larger standard deviation. The  
179 longitudinal and transverse expansions showed similar expansive behavior after 70 days, indicative of  
180 an almost isotropic DEF expansion at the stress-free condition [9].

##### 181 **(2) Expansion under restraint**

182           The expansive behaviors were strongly affected by the restraint, especially in the longitudinal  
183 direction, as shown in Figure 3(a). Furthermore, the degree of the restraint had a lesser impact on the  
184 longitudinal expansion. The final expansion of the restrained concrete ranged from 0.27% to 0.39%,  
185 corresponding to an 82–87% reduction from the free expansion. Although the asymptotic final  
186 expansion differed, the kinetics of the restrained expansion were nearly equivalent to that of the free  
187 expansion. This tendency is also reported by Bouzabata et al. for mortar [7]. The transverse expansion  
188 (Figure 3(b)) showed contradictory results to previous studies, which reported that the transverse  
189 expansion was nearly equal to free expansion [7–8]. In the present study, regardless of the degree of  
190 the restraint, the transverse expansion was considerably smaller than free expansion, with a reduction  
191 of 20–32%. One of the reasons for the reduction can be attributed to the restraint from the steel plates  
192 at the longitudinal end of the specimen (Figure 1): friction between the steel plates and the concrete  
193 specimen would influence the transverse expansion.

194           The expansive behaviors along the transverse direction at the center of the longitudinal  
195 direction (Point B) is shown in Figure 4(a) and the transverse expansions at different locations are  
196 summarized in Figure 4(b). The measurement points are illustrated in Figure 2. The expansion  
197 measured at the center of the longitudinal direction (Point B) was 30–41% larger than the those  
198 measured near the end of the longitudinal direction (Point A and C) and was 17–24% larger than the  
199 average expansion. The transverse expansions at the center (Point B) were 75–90% of the stress-free  
200 expansion (Figure 4(a)). Thiebaut et al. reported that the expansion of concrete uni-axially restrained  
201 by an internal reinforcement was around 90% of unrestrained concrete in the transverse “stress-free”  
202 direction [8]. Additionally, Bouzabata et al. showed that the expansion of mortar in the stress-free  
203 direction was not modified [7]. In the present experiment, the reduction of the transverse expansions  
204 was relatively larger than in these previous experiments. Therefore, the influence of the restraint from  
205 the friction of the steel plates on the transverse expansion would be slightly larger in this study.

206 For further information, the expansive behavior of the concrete after releasing the restraint is  
207 summarized in Appendix 1.

208

### 209 **3.2 Steel strain**

210 The following process was performed to compare the steel and concrete strain. It should be noted that  
211 the 340-mm long concrete specimen was restrained by two steel plates. The length of steel between  
212 the plates was 416 mm in length without the load cell and 516 mm with the load cell. The difference  
213 in length was due to the presence of the steel plates and washers  $((t_1 + t_2) \times 2)$ . As  
214 the displacement at the extremity of the concrete and steel was equal, the compatibility of the steel  
215 deformation should be maintained when compared with the concrete strain. Therefore, to be able to  
216 compare concrete and steel strains, the strain on the steel bar was reevaluated as follows (Figure 5).  
217 The deformation of the steel bar is the multiplication of the length of the steel bar between the nuts  
218 with its strain, given as

$$219 \quad \delta_{\text{bar}} = L_{\text{bar}} \varepsilon_{\text{bar}}, \quad (1)$$

220 where  $\delta_{\text{bar}}$  is the displacement at the extremity of the steel bar (mm),  $L_{\text{bar}}$  is the restrained length  
221 between the nuts ( $L_{\text{bar}} = 416$  mm without the load cell,  $L_s = 516$  mm with the load cell), and  $\varepsilon_{\text{bar}}$  is  
222 the measured strain of the steel.

223 The deformation of the concrete is also given by

$$224 \quad \delta_{\text{con}} = L_{\text{con}} \varepsilon_{\text{con}}, \quad (2)$$

225 where  $\delta_{\text{con}}$  is the displacement at the extremity of the concrete (mm),  $L_{\text{con}}$  is the length of the  
226 concrete prism ( $L_{\text{con}} = 340$  mm), and  $\varepsilon_{\text{con}}$  is the measured strain on the concrete surface.

227 Assuming that the deformation of the steel plates is negligible, the displacements at the ends of the  
228 concrete and steel bar should be equal ( $\delta_{\text{bar}} = \delta_{\text{con}}$ ), giving

$$229 \quad \varepsilon_{\text{bar}} = \frac{L_{\text{con}}}{L_{\text{bar}}} \varepsilon_{\text{con}}. \quad (3)$$

230 Therefore, the steel bar strain with and without the load cell is 82% and 66% of the concrete expansion  
231 strain, respectively. Therefore, the measured strain of the steel bar was reduced to these values.

232 The behavior of the calibrated steel bar strain is shown in Figure 6. Due to low insulation  
233 resistance, the strain data for the  $\phi$  13 case was not available after 95 days. In all cases, the steel strains  
234 increased linearly from around 50 days and showed a convergent trend after approximately 100 days.  
235 The final strain of the steel at 181 days was 1537  $\mu\text{m/m}$  for  $\phi$  9.2 and decreased with increasing  
236 diameter of the steel bar ( $\phi$  17: 744  $\mu\text{m/m}$ ,  $\phi$  26: 403  $\mu\text{m/m}$ ).

237

### 238 **3.3 Expansive pressure**

239 The load cells allowed direct measurements of the restraint stresses in the concrete specimens. The  
240 restraint stress represents a macroscopic evaluation of the expansive pressure. The changing pressure  
241 with time as obtained by the load cells is shown in Figure 7. The expansive pressure increases with  
242 increasing concrete expansion and steel strain. For  $\phi$  26, although a small compressive stress was  
243 induced initially, a small drift was measured at approximately 50 days. Note that such a drift could not  
244 be observed for the steel strain. This drift might have reduced the measured expansive pressure.

245

### 246 **3.4 Cracking patterns**

247 The surface crack patterns of the concrete specimens after the test are shown in Figure 8. Map cracking  
248 is observed for the stress-free expansion, with a maximum crack width of 2 mm. For the restrained  
249 specimens, the cracking patterns were somewhat consistent, with clear cracks along the longitudinal  
250 direction that were filled with white deposits. The larger the degree of the restraint, the larger the crack  
251 width and the fewer the number of cracks in the longitudinal direction. Relatively large cracks extended  
252 in the longitudinal direction, and smaller cracks extended in the transverse direction as well. As the  
253 degree of the restraint increased, the small cracks extending along the transverse direction became less  
254 than those observed for the stress-free expansion. The maximum crack width at the surface was almost

255 equal (0.4 mm) for the four restraint cases, independent of the diameter of the steel bar, and  
256 significantly lower than for the stress-free specimen (0.4 versus 2 mm for the stress-free expansion).  
257 The total crack length and crack orientation are shown in Figure 9. The crack orientation was defined  
258 as the angle from the transverse direction (cracks with an angle of  $90^\circ$  are along the longitudinal  
259 direction). The total crack length was around 800-1100 mm for all the specimens, and thus had no  
260 correlation with the degree of restraint. The work by Kchakech reported that there is a correlation  
261 between stress-free expansion and the total crack length and that the first visible cracks coincided with  
262 the inflection point of the expansion curve [29]. In this study, although the kinetic behavior of surface  
263 cracking was not evaluated, Figure 9(a) indicates that the kinetic relation between expansion and the  
264 total crack length under restraint is different from stress-free one. In contrast, the crack orientation was  
265 strongly influenced by the degree of constraint: the unrestrained specimen demonstrated perfectly  
266 isotropic cracking with very few dispersions along all directions, and specimens with the largest  
267 restraint ( $\phi 17$  and  $\phi 26$ ) exhibited more than half their cracks in the  $60\text{-}90^\circ$  direction. This demonstrates  
268 a key anisotropy in the cracking even if cracks in all directions can be observed.

269         The inner crack pattern of the concrete specimen after the test in the transverse and  
270 longitudinal directions is shown in Figure 10 and Figure 11, respectively. In the figures, the area where  
271 the concrete surface is uneven due to aggregate debonding is encircled by red dotted lines; since the  
272 concrete was heavily damaged by DEF expansion, it was difficult to cut the specimens without  
273 inducing any damage. The fluorescence can be observed for all cases, especially around the coarse  
274 aggregate, which is generally termed as a “gap”. The gaps are opening providing evidence of DEF  
275 expansion. The fluorescence was also observed in pores and cracks. The width of the gap is the largest  
276 for the stress-free specimen for both directions. For the restrained specimens, no distinct difference  
277 could be found. It is known that the gap forms as a result of expansion and is related to the magnitude  
278 of expansion: the larger the expansion, the larger the width of the gap [30]. The trends in the inner  
279 crack pattern seem consistent with the results of the expansion test. At the surface, fine cracks in the

280 transverse direction were reduced according to their degree of restraint. It should be noted, however,  
281 that the cracking patterns for  $\phi$  17 and  $\phi$  26 did not change significantly. For internal cracks, no clear  
282 difference with varying degree of restraint was observed for gaps and cracks, although there is a  
283 considerable difference between the restrained specimens and the stress-free expansion. As for stress-  
284 free specimens, the maximum width around the coarse aggregate reached 1.0 mm. It could be  
285 hypothesized that such a large width might be attributable to the opening during the operations  
286 performed for the observation such as cutting and impregnation; but this was confirmed to be of the  
287 same order of magnitude by nondestructive x-ray micro computed tomography (CT) on a cylinder  
288 specimen with almost the same expansion (0.9 mm in width for an expansion of 2.17%, see Appendix  
289 2), suggesting that the width of 1.0 mm is attributed to DEF expansion. The width around the coarse  
290 aggregate is reduced to approximately 300  $\mu$ m for the restrained specimens. For the width of the gap  
291 across the cross-section along the longitudinal and transverse directions, no apparent tendency between  
292 the specimens can be found.

293

## 294 **4. Discussion**

### 295 **4.1 Anisotropy of restrained DEF expansion**

296 The relationship between longitudinal and transverse expansion is illustrated in Figure 12. As  
297 described above, the stress-free expansion demonstrated nearly isotropic behavior while the stressed  
298 concrete demonstrated strong anisotropy. In each case, there is a quasi-linear relationship between the  
299 longitudinal and transverse expansions. Anisotropic coefficients (longitudinal /transverse expansion)  
300 calculated from the average expansions are within 0.14–0.22 for the restrained specimens, similar to  
301 the results of previous studies [7–8]. Note that the anisotropic coefficients are within 0.09–0.19 when  
302 the transverse expansion at Point B was used for calculation. The anisotropy of the expansion is  
303 confirmed by the quantification of the orientation of the induced cracks (Figure 10).

304 To compare the results with those of previous studies [7–8], the ratio of the cross-sectional  
305 area of the steel bar and the concrete,  $A_s/A_c$ , was calculated. Figure 13 shows the “expansion ratio”  
306 versus  $A_s/A_c$ , where the expansion ratio is defined by the decrease of longitudinal expansion due to  
307 the steel restraint (ratio of the expansion of the restrained concrete to the stress-free expansion). For  
308 comparison, results for ASR expansion from the literature are also shown in the figure [16, 21]. Note  
309 that, for the data from Mohammed et al., only the cases with end plates are plotted as expansions  
310 measured on specimens without steel plates can be affected by the loss of a portion of the steel-concrete  
311 bonding for high degrees of expansion. The expansion ratio is greatly influenced by  $A_s/A_c$ , irrespective  
312 of the cause of expansion (ASR or DEF). Only a small  $A_s/A_c$  ratio, and thus a small restraint rigidity,  
313 drastically changes the expansion in the restrained direction, while the degree of restraint has a minor  
314 impact when  $A_s/A_c$  is over 1.0%. Although results for the restrained cases with  $A_s/A_c$  below 0.5 is not  
315 available for DEF, the general trend for the reduction in longitudinal expansion due to the restrained  
316 expansion as measured for the mortars and concrete seems to be similar between DEF and ASR. The  
317 relationship between  $A_s/A_c$  and anisotropy coefficients is summarized in Figure 14. Although the  
318 chemical mechanisms of expansion are completely different between ASR and DEF, the mechanical  
319 response of concrete to these two types of internal expansion seems similar. Since the expansion  
320 transfer cannot be found for DEF as for ASR (Figure 3, 12), the influence of the restraint on the  
321 expansion along the restrained direction is larger for DEF. Thus, a similar quantitative trend to the  
322 expansion ratio can be found: even a small degree of restraint can greatly reduce the anisotropic  
323 coefficient. The anisotropic coefficient does not reach zero even when the concrete is highly restrained;  
324 the minimal ratio of approximately 0.2 corresponds to the longitudinal expansion necessary to obtain  
325 a sufficient longitudinal compressive stress to arrest expansion along this direction. The results in this  
326 study are consistent with those of previous studies on mortar and concrete submitted to DEF and ASR  
327 [7–8, 16]. These results also increase the domain of validity for the evolutions of the expansion and  
328 anisotropy ratios in the case of concrete reinforced by high steel ratios and submitted to DEF.

329

## 330 **4.2 Expansive pressure**

331 The strains measured on the steel bars can be used to evaluate the expansive pressure and thus be  
332 compared to the direct measurement of pressure from the load cell. First, the expansive pressure was  
333 calculated from the steel strain as shown in Figure 15. Note that the raw data of the steel bar strain was  
334 used “without calibration” for the pressure calculation since the stress induced by the steel bar is  
335 reflected by the actual strain of the steel bar. Additionally, the relationship between the load-cell  
336 measurement and the calculation is summarized in Figure 16. The trend in the calculation results is  
337 consistent with the measurement ( $\pm 0.25$  MPa) except for the  $\phi 26$  case. In this case, above 0.5 MPa  
338 of measured pressure, the measurement is around 65% of the calculated pressure. While the steel was  
339 located in the center of the concrete and the average expansion of the concrete was measured, the load  
340 cell requires a uniform stress acting on the bearing area of the load cell. However, DEF expansion is  
341 not uniform across the cross-section, and thus the eccentric stress deriving from the difference of  
342 expansion across the cross-section might affect the measurement results of the load cell. This may  
343 have possibly occurred due to the presence of the small interspace or the deformation of the steel plates.  
344 Such a loss of expansive pressure may have occurred for the  $\phi 17$  case, where slip-like behavior was  
345 observed at 2.0 MPa. However, it should be noted that the slope before and after the slip is equal so  
346 the lost pressure seems to be small (possibly 0.5 MPa).

347 Furthermore, assuming compatibility between the concrete ( $\epsilon_c$ ) and steel ( $\epsilon_s$ ) strains, the  
348 expansive pressure can be calculated from the expansion strain of the concrete. As a result, the  
349 expansive pressure calculated from the concrete strain and the Young’s modulus of the steel bar ranges  
350 from 5.7 to 20.7 MPa, which is unrealistic as compared to previous studies [7–8]. The unrealistic  
351 evaluation of pressure from the concrete strain may result from structural deformation during  
352 expansion as discussed in the following section. Actually, according to the experiment by Thiebaut et  
353 al., 14.5 MPa of applied compressive stress contracts the concrete without any expansion [8]. A



354 summary of  $A_s/A_c$  versus expansive pressure, including the results of previous studies [7–8], is  
355 illustrated in Figure 17. Complementary results for DEF under bi-axial restraint are presented in  
356 Appendix 3. These results are not presented in the main body of this study as they were obtained for a  
357 different concrete under different environmental conditions; however, they can provide interesting  
358 insight on multi-axial restraint, particularly in terms of expansive pressure. In the present study, the  
359 expansive pressures measured by the load cell and calculated from the steel strain are generally  
360 consistent. At an  $A_s/A_c$  of 6.0, the expansive pressure measured by the load cell is lower than the  
361 calculated pressure due to the afore-described mechanism. The results of Thiebaut et al. show the  
362 greatest expansive pressure as calculated from the concrete surface expansion despite a lower  $A_s/A_c$ .  
363 However, the data of Thiebaut et al. is within the range of the expansive pressure resulting from  
364 external sulfate attack [27]. It should also be noted that, in the experiment by Thiebaut et al. [8], the  
365 steel bar was embedded in concrete, while in the present study and the experiment by Bouzabata, an  
366 external restraint system was used without bonding, so the effect of bonding between concrete and the  
367 steel bar might have an impact.

368 As for the ASR expansion of concrete under stress as measured by Kagimoto et al., the  
369 expansive pressure for different degrees of restraint ranged from 0.3 to 2.6 MPa [16]. Additionally, for  
370 the experiment by Berra et al., the expansive pressure of concrete was measured for different mixes  
371 and initial stresses, with a single restraint condition considered [15]. As a result, the expansive pressure  
372 was between 0.45-5.6 MPa (for concrete with stress-free expansion between 0.04 and 0.5%). As for  
373 the mortar with two different aggregates, Kawamura and Iwahori measured expansive pressures  
374 between 0.4 and 4.5 MPa [23]. The relationship between the expansive pressure obtained for expansion  
375 under restraint conditions and the unrestrained ultimate expansion is summarized in Figure 18,  
376 including the case of ASR with DEF data. No obvious tendency can be found, which may be due to  
377 the differences of restraint levels between experiments. However, the level of macroscopic pressure  
378 obtained for DEF and ASR under restraint conditions is below 6 MPa for free swelling until 2.5%,

379 regardless of the origin of expansion. Comparing the expansive pressure from ASR and DEF, it is  
380 notable that the expansive pressure is almost on the same order of magnitude as the ASR pressure,  
381 ranging from 0.3 to 6 MPa, despite a larger free DEF expansion as compared to ASR. The stress-free  
382 expansion due to DEF is one order of magnitude greater than that of ASR. Nevertheless, it is possible  
383 that a small degree of restraint is sufficient to reduce DEF expansion. In laboratory experiments,  $A_s/A_c$   
384 is generally higher than that of real structures, and thus more investigations will be necessary. However,  
385 it should be noted that the expansion cannot be perfectly prevented by the passive restraint as sufficient  
386 expansion is needed to induce significant compressive stresses. Active application of a compressive  
387 stress such as prestressing may be necessary to prevent any expansion.

388

#### 389 **4.3 Steel and concrete strains**

390 The relationship between the expansion of the concrete surface and the steel strain is shown in Figure  
391 19. Here, the strain of the steel bar is calibrated according to Eq. (1) – (3). The strain measured on the  
392 steel bar was not equal to the expansion strain measured on the external surface of concrete. The ratio  
393 of the steel strain to the expansion strain of the concrete at the end of the test was the highest for  $\phi$  9.2  
394 (42%) and the lowest for  $\phi$  26 (14%). There may be several reasons for the discrepancy between the  
395 concrete expansion and steel strain. The first consideration is the rigidity of the load cell. In the  
396 discussion between Kagimoto and Hansen [31–32], the stiffness of the testing apparatus has a critical  
397 impact on the expansive pressure as experimentally measured for ASR. This is also the case for DEF  
398 expansion. To evaluate the impact of the load cell on the steel strain, all deformation mechanisms were  
399 evaluated:

400 - the deformation of load cell at 30 kN of compression (corresponding to 3.4 MPa of expansive  
401 pressure) is theoretically 0.009 mm.

402 - the steel plates were deformed by compression, which should be approximately 0.001 mm.

403 For instance, as for the  $\phi 9.2$  case, considering the final length after 0.15% expansion, the  
404 deformation of the steel bar is 0.63 mm. Therefore, the longitudinal deformation of the restraint  
405 apparatus after final expansion is 0.62 mm ( $0.062 = 0.63 - 0.009 - 0.001$  mm). The expansion of the  
406 concrete calculated from the deformation of the restraint system would be 0.18%, which is around half  
407 that of the measured expansion at the concrete surface.

408 Second, there may be possible corrosion of the steel plates. This corrosion would be almost  
409 negligible since the steel plates and steel bar were protected by sacrificial anodes (Mg alloy) and visible  
410 corrosion could not be found after the test. Finally, there is the mechanical instability of concrete  
411 specimens with holes inside them. The minimum thickness of the concrete is 31 mm. Compared to  
412 massive specimens such as those used in the experiment performed by Thiebaut et al. [8], the specimen  
413 might deform and become barrel shaped. In this case, the steel strain could be smaller than the  
414 expansion strain of the concrete surface, as concrete shows considerable out-of-plane deformation. For  
415 instance, according to the experiment by Müllauer et al. [27], in which a stainless steel bar was  
416 embedded in a thin-walled mortar specimen, some of the mortar specimen showed buckling damage.  
417 Although visible buckling could not be observed in Figure 8–11, this mechanism may explain why the  
418 ratio of the steel strain to the expansion strain of the concrete decreases with increasing steel bar  
419 diameter. When the diameter of the steel bar increases, the compressive stress acting on the concrete  
420 specimen is higher, resulting in pronounced out-of-plane deformation despite the small expansion.  
421 Consequently, a smaller steel strain is obtained in the highly reinforced specimen.

422 Many studies have assumed perfect bonding between steel and expansive concrete. However,  
423 typically, the expansion strain is only measured on the external surfaces of the concrete. Few  
424 experimental works have compared the external concrete strain and the reinforcement steel strain  
425 measurements as in the present study and no possible comparison is available. The choice of a  
426 specimen with a hole may have led to structural buckling and thus resulted in the difference in the

427 strains measured on concrete and steel in the present study. To improve this analysis, future numerical  
428 analyses are planned to model the present experimentation with a mesoscale modeling [33].

429

#### 430 **4.4 Reduction in expansion in the presence of the restraint**

431 Considerable reduction in longitudinal expansion was found in the presence of the restraint. There may  
432 be two possible primary mechanisms: the reduced expansive potential of DEF and enhanced creep  
433 strain. In this study, the expansive potential of DEF as modified by the restraint is focused on. The  
434 relationship between imposed DEF expansion and restrained expansion may be given by Eq. (4), with  
435 tension (expansion) defined as positive:

$$436 \quad \varepsilon_{\text{res}} = \varepsilon_e + \varepsilon_{\text{cr}} + \varepsilon_{\text{imp}}, \quad (4)$$

437 where  $\varepsilon_{\text{imp}}$  is imposed DEF expansion,  $\varepsilon_e$  is the elastic strain from compression (induced by the  
438 restraint),  $\varepsilon_{\text{cr}}$  is the creep strain under restraint, and  $\varepsilon_{\text{res}}$  is the expansion strain under restraint. The  
439 strain measured before and after releasing the restraint is considered as elastic strain ( $\varepsilon_e$ ). In this case,  
440 the Young's modulus can be calculated from the expansive pressure measured by the load cell ( $\sigma_{\text{DEF}}$ )  
441 and the differential elastic strain ( $\varepsilon_e$ ) between before and after releasing the restraint. Note that the  
442 Young's modulus was measured from stress-free cylindrical specimens (see Section 2.1,  $E_c = 1.2$   
443 GPa). The creep strain can be calculated assuming that the creep coefficient ( $\varepsilon_{\text{cr}}/\varepsilon_e$ ) is constant at 2  
444 regardless of the expansion.

445 The calculated result is shown in Table 4. From the calculation, the imposed DEF expansion  
446 was reduced from the stress-free expansion by approximately 80%. The estimated Young's modulus  
447 is seven to nine times higher than that of the stress-free specimen after the test. It is notable that DEF  
448 expansion under restraint is reduced significantly. In this calculation, creep was assumed to be not  
449 modified by DEF. Therefore, although it is difficult to conclude which mechanism is dominant for the  
450 reduction in DEF expansion under the restraint condition, an approach considering a reduction in DEF  
451 expansion under restraint may be possible for further modeling. Further research is required to quantify

452 the relationship between stress and DEF expansion under stress. Besides, the results in this paper  
453 clearly indicated a possibility that a small degree of restraint is sufficient to reduce DEF expansion.  
454 Whilst this study showed the DEF expansion under uni-axial restraint (bi-axial restraint as well in  
455 Appendix), the effect of three-dimensional restraint on DEF expansion, which is more likely to be real  
456 structure, is also necessary to be investigated.

457

## 458 **5. Conclusions**

459 The influence of restraint on expansion, expansive pressure, and cracking patterns due to delayed  
460 ettringite formation (DEF) in concrete was experimentally evaluated and compared to a large number  
461 of experimental results on the effect of restraint on internal swelling reaction (ASR and DEF). The  
462 conclusions can be summarized as follows:

463 (1) Longitudinal expansion was considerably reduced (82–87%) in the presence of restraint while the  
464 reduction in the transverse expansion was 20–32%. The reduction in the transverse expansion  
465 might be attributable to the restraint provided by the steel plates at the end of the specimen. The  
466 decrease in longitudinal expansion was consistent with experimental results in the literature  
467 obtained for mortar. The present experimental results provide quantitative conclusions for concrete  
468 and for intermediate degrees of restraint.

469 (2) For the first time, expansion pressure was evaluated directly for DEF expansion under restraint.  
470 The pressure measured by the load cell was 1.9–3.9 MPa, which is nearly consistent with those  
471 calculated from the steel bar strain. The expansive pressure calculated from the strain of the  
472 concrete surface was significantly higher than those directly measured with the load cell, possibly  
473 due to out-of-plane deformation of the holed specimen. The expansive pressure of DEF was almost  
474 of the same order of magnitude as for ASR expansion, despite larger free DEF expansion than  
475 ASR.

476 (3) This experimental work leads to important results concerning the quantification of cracks on the  
477 surface and the observations of inner cracks in concrete specimens submitted to DEF under  
478 restraint:

- 479 a. The total length of surface cracking was independent of the degree of the restraint,
- 480 b. The orientation of cracks was isotropic for concrete subjected to DEF in stress-free  
481 expansion,
- 482 c. The anisotropy of cracks due to restrained DEF expansion was quantified in terms of  
483 the cracks distribution,
- 484 d. The inner crack pattern was similar for the restraint case while large gap formation was  
485 observed for the stress-free case.

486 The quantification of cracks of DEF-damaged concrete is an important issue for the management  
487 of affected structures as cracks affect the supply of water in the material and can accelerate the  
488 damage of concrete in combination with other external attacks.

489

#### 490 **Acknowledgements**

491 Part of this work was financially supported by the Japan Society for the Promotion of Science (JSPS,  
492 No. 20H02227). The authors also would like to thank Dr. Badreddine Kchakech for providing advice  
493 on the crack pattern analysis.

494

#### 495 **Appendix 1: Expansive behavior of concrete after releasing the restraint**

496 After 181 days, the apparatus for the restraint was removed from the concrete specimen. Then, using  
497 two specimens that were not used for crack observation, the expansion of the concrete specimen after  
498 stress release was continuously measured. The expansion curves of the concrete specimens after  
499 releasing the restraint are given in Figure A1. The longitudinal and transverse expansions gradually

500 increased with time. No trend in the increased expansion after releasing the restraint can be observed.  
501 The trends seem to be similar for the four restraints.

502           The relationship between the longitudinal and transverse expansions is illustrated in Figure  
503 A2. In this figure, the expansion was normalized by subtracting the final expansion before releasing  
504 the restraint. As for the stress-free specimen, an almost isotropic expansion can be confirmed (a ratio  
505 of 1.14 between transverse and longitudinal expansions). In contrast, it was found that the curves for  
506 the stress-released specimens (formerly restrained specimens) are concave up when the longitudinal  
507 expansion is less than 0.15%, with the longitudinal expansions then mostly linear with transverse  
508 expansion. The larger longitudinal expansion below 0.15% longitudinal expansion might be  
509 attributable to elastic deformation and creep recovery after releasing the restraint. Above 0.15%, the  
510 ratios of the transverse expansions to the longitudinal expansions are 2.0-2.6 for the stress-released  
511 specimens, suggesting an anisotropic expansion of the concrete even after releasing stresses. This  
512 might be due to anisotropic damage induced during the restraint. In actual structures affected by DEF  
513 expansion, the stress states are complex, and thus care must be taken when performing an expansion  
514 test on concrete core extracted from an already-damaged structure: when only longitudinal expansion  
515 is measured, the potential residual expansion may be underestimated.

516

## 517 **Appendix 2: Internal cracking pattern captured by x-ray microtomography scanning**

518 A 100-mm in diameter cylindrical specimen 200 mm in length after the expansion test was used for  
519 nondestructive x-ray microtomography scanning (X- $\mu$ CT). Expansion of the specimen after the test  
520 was 2.17%. The ScanXmate-D200RSS900 x-ray CT scanner system located at the Port and Airport  
521 Research Institute in Yokosuka, Japan, was used for the investigation. The maximum voltage and  
522 current of the x-ray tube are 225 kV and 0.6 mA, respectively. The transmitted x-rays are detected by  
523 a 418 by 418 mm flat panel with a resolution of 3008 by 3008 pixels.

524 The x-ray CT image of the concrete cylindrical specimen is shown in Figure A3. The gaps  
525 around the aggregate can be easily observed. The maximum width of the gap is estimated as 0.9 mm,  
526 which is consistent with the observation using fluorescent epoxy resin.

527

### 528 **Appendix 3: Expansion of concrete under bi-axial restraint**

529 To evaluate the expansive behavior of concrete under bi-axial restraint, the following experiments  
530 were carried out in Kansai University.

#### 531 **A3.1 Experiments**

##### 532 **A3.1.1 Test specimens**

533 Cylindrical concrete specimens surrounded by a stainless cylindrical tube with a 100-mm diameter, as  
534 shown in Figure A4, were used for DEF expansion test under bi-axial restraint. Three degrees of  
535 restraint were considered by changing the tube thicknesses. The thicknesses of the stainless tube were  
536 0.25, 0.5, and 1.0 mm, giving restraint ratios along the circumferential direction of 0.5, 1.0, and 2.0%,  
537 respectively. Apart from the uni-axial restraint condition, the DEF concrete expansion in the  
538 circumferential direction was bi-axially restrained by the tube. In contrast, the longitudinal expansion  
539 was restrained by the friction between the concrete and the stainless tube. The concrete was actually  
540 subjected to tri-axial restraint; however, the degree of restraint in the longitudinal direction was lower,  
541 as shown in A3.2.1. Therefore, in this study, this experimental case is regarded as “bi-axial restraint”.  
542 Hereafter, the specific test cases are denoted by the thickness of the stainless tube, e.g., “t0.25”. Three  
543 cylinders were prepared for the stress-free, t0.5, and t1.0 specimens while two cylinders were prepared  
544 for the t0.25 specimens. The test specimen details are described as follows.

545 The mixture proportion of the concrete is shown in Table A1. The cement was Ordinary  
546 Portland Cement (Type I Portland Cement), which differs from the cement used for the samples in the  
547 main body of this study (see Table 2). The SO<sub>3</sub> content of the cement was 2.17%. A portion of the  
548 cement was replaced by a K<sub>2</sub>SO<sub>4</sub> reagent so that the total SO<sub>3</sub> content was increased to 8.8% of the



549 cement by weight.  $K_2SO_4$ . Non-reactive sand and gravel were used for the aggregate and the water-to-  
550 cement ratio including  $K_2SO_4$  was 0.57.

551 The concrete was directly cast into the stainless tube. After casting, the specimens were  
552 subjected to heat-curing following a similar curing cycle to the uni-axial restraint test (see Section 2.1):  
553 starting from four hours after casting, heat the specimen to 90 °C at a rate of +35.4 °C/h, maintain for  
554 12 h, then cool to 20 °C at a rate of -34.9 °C/h.

555

### 556 **A3.1.2 Expansion test**

557 After heat curing, the specimens were subjected to an expansion test in which the specimens were  
558 immersed for 378 days in water kept at 20 °C. It should be noted that the stress-free specimen was  
559 wrapped by waterproof aluminum tape with acyl adhesion to maintain the same moisture conditions  
560 as the restraint specimens.

561 The length changes of the concrete in the axial direction (length of 200 mm) were measured  
562 by a linear gauge with a precision of 0.0005 mm. The studs for the measurement were installed on the  
563 end surfaces in the longitudinal direction of the cylindrical specimen. Strains along the axial and  
564 circumferential directions of the stainless tube were also measured by strain gauges (length of 5 mm)  
565 attached to the center of the stainless tube. Initial measurements were performed at twenty-four hours  
566 after casting.

567

## 568 **A3.2 Results and discussion**

### 569 **A3.2.1 Expansion measured from the concrete**

570 The concrete expansions due to DEF in the longitudinal direction are illustrated in Figure A5. Error  
571 bars in the figure are the standard deviations of the measured expansions. In the stress-free condition,  
572 the onset of expansion was around 20 days and the expansion exceeded 0.5% at 115 days. Finally, the  
573 expansion was 0.78% at 378 days. When the concrete was restrained by the thin stainless tube, the

574 longitudinal expansion of t0.25, t0.05, and t0.10 reduced to 0.36%, 0.19%, and 0.23%, respectively.  
575 While the longitudinal expansion was reduced by the stainless tube, the reduction was not significant  
576 at approximately 24–47% of the stress-free expansion. This is because the expansion in the  
577 longitudinal direction was restrained only by friction. The longitudinal expansion of t1.00 was slightly  
578 larger than that of t0.50 from 115 days. While this indicates a possible expansion transfer of DEF  
579 expansion, this possibility would be rejected due to the reason described in 3.2.2.

580

### 581 **A3.2.2 Strains measured from the stainless tube**

582 Steel tube strains due to DEF in the longitudinal and circumferential directions are illustrated in Figure  
583 A6. It is found that DEF expansion is nearly isotropic, so the circumferential strain can be compared  
584 with the longitudinal expansion of the stress-free concrete. The circumferential expansion (Figure  
585 A6(b)) was drastically reduced in the presence of the stainless tube. All the cases demonstrated an  
586 expansion 10% less than that of the stress-free case. For “t1.00”, the expansion was only 2% of the  
587 stress-free expansion. The longitudinal strain of the stainless tube was within 0.015% and 0.031%: the  
588 expansive pressure of concrete is transferred to the stainless tube by means of friction, so the strain is  
589 quite small. This is the reason that the concrete specimens were regarded as essentially being in a bi-  
590 axial restraint condition. Indeed, slip-like behaviors of the longitudinal strains can be observed in  
591 Figure A6. In Figure A5, the longitudinal expansion of t1.00 was slightly larger than that of t0.50. This  
592 tendency might be explained by the friction. The longitudinal tube strain of t0.50 was two to three  
593 times higher than t1.00, suggestive of larger friction forces acting on the concrete, in which greater  
594 friction reduces the longitudinal expansion. Additionally, expansions in the longitudinal and  
595 circumferential directions were reduced in the presence of the stainless tube, leading to a significant  
596 reduction in volumetric expansion. Therefore, it can be concluded that expansion transfer would not  
597 be observed even in the presence of the bi-axial restraint.

598           The relationship between the longitudinal expansion of the concrete and the circumferential  
599 strain is shown in Figure A7. A similar tendency was found for the bi-axial restraint condition, in that  
600 the circumferential tube strain is significantly lower than the longitudinal expansion of the concrete.  
601 The ratios of the circumferential tube strain to the longitudinal expansion of the concrete are 0.05–  
602 0.23, which are similar to those observed in the uni-axial restraint test.

603           Expansive pressure as a function of  $A_s/A_c$  is illustrated in Figure A8, which includes the uni-  
604 axial restraint data presented in Figure 16. Expansive pressure was calculated from the circumferential  
605 strain based on the elastic mechanical model [13, 34]. In this calculation, creep, damage (reduction in  
606 Young's modulus), and expansion transfer were not considered. The Young's modulus of the concrete  
607 and stainless tube was 35.0 GPa (rough estimation) and 193 GPa (from a material test result),  
608 respectively. At 378 days, the calculated expansive pressure, as well as the confinement pressure from  
609 the stainless tube, in the circumferential direction for  $t_0.25$ ,  $t_0.50$ , and  $t_1.00$  was 0.76 MPa, 1.12 MPa,  
610 and 0.76 MPa, respectively. These results indicate that DEF expansion is quite sensitive to compressive  
611 stress. As a result, the bi-axial restraint experiment demonstrated lower expansive pressure. The results  
612 of the bi-axial restraint test also suggest that the expansive pressure of DEF concrete under the restraint  
613 condition is nearly equal or less than that of ASR concrete.

614

## 615 **References**

- 616 [1] H.F.W. Taylor, C. Famy and K.L. Scrivener: Delayed ettringite formation, *Cement and Concrete*  
617 *Research*, Vol. 31, pp. 683–693, 2001.
- 618 [2] R.J. Flatt and G.W. Scherer: Thermodynamics of crystallization stresses in DEF, *Cement and*  
619 *Concrete Research*, Vol. 38, pp. 325–336, 2008.
- 620 [3] A. Sellier, S. Multon: Chemical modelling of Delayed Ettringite Formation for assessment of  
621 affected concrete structures, *Cement and Concrete Research*, Vol.108, pp. 72–86, 2018.

- 622 [4] R.-P. Martin, O. O. Metalssi, F. Toutlemonde: Importance of considering the coupling between  
623 transfer properties, alkali leaching and expansion in the modelling of concrete beams affected by  
624 internal swelling reactions, *Construction and Building Materials*, Vol. 49, pp. 23–30, 2013
- 625 [5] M. M. Karthik, J. B. Mander, S. Hurlbaas: Deterioration data of a large-scale reinforced concrete  
626 specimen with severe ASR/DEF deterioration, *Construction and Building Materials*, Vol. 124, pp.  
627 20–30, 2013.
- 628 [6] O. Omikrine-Metalssi, B. Kchakech, S. Lavaud & B. Godart, A new model for the analysis of the  
629 structural/mechanical performance of concrete structures affected by DEF - Case study of an  
630 existing viaduct, *Structural Concrete*, 2016.
- 631 [7] H. Bouzabata, S. Multon, A. Sellier, and H. Houari: Effects of restraint on expansion due to  
632 delayed ettringite formation, *Cement and Concrete Research*, Vol. 42, pp. 1024–1031, 2012.
- 633 [8] Y. Thiebaut, S. Multon, A. Sellier, L. Lacarrière, L. Boutillon, D. Belili, L. Linger, F. Cussigh, and  
634 S. Hadji: Effects of stress on concrete expansion due to delayed ettringite formation, *Construction  
635 and Building Materials*, Vol. 183, pp. 626–641, 2018.
- 636 [9] H. Bouzabata, S. Multon, A. Sellier, and H. Houari: Swellings due to alkali-silica reaction and  
637 delayed ettringite formation: Characterisation of expansion isotropy and effect of moisture  
638 conditions, *Cement and Concrete Composites*, Vol. 34, pp. 349–356, 2012.
- 639 [10] A.E.K. Jones, L.A. Clark: The effects of restraint on ASR expansion of reinforced concrete,  
640 *Magazine of Concrete Research*, Vol. 174, pp. 1–13, 1996.
- 641 [11] C. Larive: Apports combinés de l’expérimentation et de la modélisation à la compréhension de  
642 l’alcali-réaction et de ses effets mécaniques, *Laboratoire Central des Ponts et Chaussées (Edt.),  
643 Ouvrage d’Art, Rapport OA 28*, 1998
- 644 [12] C. Gravel, G. Ballivy, K. Khayat, M. Quirion, M. Lachemi: Expansion of AAR concrete under  
645 triaxial stresses: simulation with instrumented concrete block, in: *Proc. 11th Int. Conf. Alkali  
646 Aggreg. React.*, Québec, Canada, pp. 949–958, 2000.

- 647 [13]S. Multon, F. Toutlemonde: Effect of applied stresses on alkali-silica reaction-induced expansions,  
648 Cement and Concrete Research, Vol. 36, pp.912–920, 2006.
- 649 [14]C.F. Dunant, K.L. Scrivener: Effects of uniaxial stress on alkali-silica reaction induced expansion  
650 of concrete, Cement and Concrete Research, Vol. 42, pp. 567–576, 2012.
- 651 [15]M. Berra, G. Faggiani, T. Mangialardi, and A.E. Paolini: Influence of stress restraint on the  
652 expansive behaviour of concrete affected by alkali-silica reaction, Cement and Concrete Research,  
653 Vol. 40, pp. 1403–1409, 2010.
- 654 [16]H. Kagimoto, Y. Yasuda, M. Kawamura: ASR expansion, expansive pressure and cracking in  
655 concrete prisms under various degrees of restraint, Cement and Concrete Research, Vol. 59, pp.  
656 1–15, 2014.
- 657 [17]B.P. Gautam, D.K. Panesar, S.A. Sheikh, F.J. Vecchio: Multiaxial Expansion-Stress Relationship  
658 for Alkali Silica Reaction-Affected Concrete, ACI Materials Journal, Vol. 114, pp.171–184, 2017.
- 659 [18]N.W. Hayes, Q. Gui, A. Abd-elssamd, Y. Le Pape, A.B. Giorla, S. Le Pape, E.R. Giannini, Z.J.  
660 Ma, L. Charpin, A. Ehrlacher, N.W. Hayes, Q. Gui, A. Abd-elssamd, Y. Le Pape: Monitoring  
661 alkali-silica reaction significance in nuclear concrete structural member s, Journal of Advanced  
662 Concrete Technology, Vo. 16, pp. 179–189, 2018.
- 663 [19]J. Liaudat, I. Carol, C.M. López, V.E. Saouma: ASR expansions in concrete under triaxial  
664 confinement, Cement and Concrete Composites, Vol. 86, pp. 160–170, 2018.
- 665 [20]S. Kongshaug, O. Oseland, T. Kanstad, M.A.N. Hendriks, E. Rodum, G. Markeset: Experimental  
666 investigation of ASR-affected concrete – The influence of uniaxial loading on the evolution of  
667 mechanical properties, expansion and damage indices, Construction and Building Materials, Vol.  
668 245, 118384, 2020.
- 669 [21]T. U. Mohammed, H. Hamada, and T. Yamaji: Relation between strain on surface and strain over  
670 embedded steel bars in ASR affected concrete members, Journal of Advanced Concrete Research,  
671 Vol. 1, No. 1, pp. 76–88, 2003.

- 672 [22]P. Morenon, S. Multon, A. Sellier, E. Grimal, F. Hamon and E. Bourdarot: Impact of stresses and  
673 restraints on ASR expansion, *Construction and Building Materials*, Vol.140, pp. 58–74, 2017.
- 674 [23]M. Kawamura and K. Iwahori: ASR gel composition and expansive pressure in mortar under  
675 restraint, *Cement and Concrete Composites*, Vol. 26, pp. 47–56, 2004.
- 676 [24]R.G. Pike: Pressures developed in cement pastes and mortars by the alkali-aggregate reaction,  
677 *HRB Bulletin*, Vol. 172, pp. 34–36, 1967.
- 678 [25]C.F. Ferraris, J.R. Clifton, E.J. Garboczi and F.L. Davis: Stress due to alkali-silica reactions in  
679 mortars, *Mechanisms of Chemical Degradation of Cement-based Systems*, K.L. Scrivener and J.F.  
680 Young (Eds.), E & FN Spon, pp. 75–82, 1997.
- 681 [26]M. Fujii, K. Kobayashi, K. Kojima and H. Mehara: The static and dynamic behavior of reinforced  
682 concrete beams with cracking due to alkali–silica reaction, in: *Proc. 7th Int. Conf. Alkali Aggreg.*  
683 *React.*, Ottawa, Canada, pp. 126–130, 1987.
- 684 [27]W. Müllauer, R. E. Beddoe, and D. Heinz: Sulfate attack expansion mechanisms, *Cement and*  
685 *Concrete Research*, Vol. 52, pp. 208–215, 2013.
- 686 [28]M. Alnagar, G. Cusatis, and G. Di Luzio: Lattice Discrete Particle Modeling (LDPM) of Alkali  
687 Silica Reaction (ASR) deterioration of concrete structures, *Cement and Concrete Composites*, Vol.  
688 41, pp. 45–59, 2013.
- 689 [29]Badreddine Kchakech: Etude de l'influence de linfluence de l'échauffement subi par un béton sur  
690 le risque d'expansions associées à la Réaction Sulfatique Interne, Ph. D thesis of Universite Paris-  
691 Est, 2015 (in French)
- 692 [30]J. Skalny, V. Johansen, N. Thaulow and A. Palomo: DEF: As a form of sulfate attack, *Materiales*  
693 *de Construction*, Vol. 46, pp.5–29, 1996
- 694 [31]S.G. Hansen and D. Skou: Discussion on “ASR expansion, expansive pressure and cracking in  
695 concrete prisms under various degrees of restraint”, *Cement and Concrete Composites*, Vol. 79,  
696 pp. 419–421, 2016.

- 697 [32]H. Kagimoto, Y. Yasuda and M. Kawamura: Reply to the discussion by S.G. Hansen of the paper  
698 “ASR expansion, expansive pressure and cracking in concrete prisms under various degrees of  
699 restraint”, *Cement and Concrete Composites*, Vol. 79, pp. 422–423, 2016.
- 700 [33]T. Miura, H. Nakamura and Y. Yamamoto: Impact of origination of expansion on three-  
701 dimensional expansion crack propagation process due to DEF evaluated by mesoscale discrete  
702 model, *Construction and Building Materials*, Vol. 260, 119911, 2020.
- 703 [34]Y. Kawabata, J.-F. Seignol, R.-P. Martin and F. Toutlemonde: Macroscopic chemo-mechanical  
704 modeling of alkali-silica reaction of concrete under stresses, *Construction and Building Materials*,  
705 Vol. 137, pp. 234–145, 2017.
- 706

1

**Table 1 Summary of experimental conditions in previous studies related to expansive pressure.**

	Bouzabata et al. [7]		Thiebaut et al. [8]		Müllauer et al. [27]				
Mortar/Concrete	Mortar		Concrete		Mortar (two cements)				
Specimen size	40 × 40 × 160 mm		100 × 100 × 500 mm		φ30 × t2.5 × L70 mm (thin wall)				
Expansion mechanism	DEF, no ESA		DEF, no ESA		ESA under Na <sub>2</sub> SO <sub>4</sub> solution (SO <sub>4</sub> <sup>2-</sup> : 1.5 & 30 g/L)				
Longitudinal direction									
Restraint condition	External restraint by four threaded stainless steel bars		Internal restraint by a stainless steel bar with interfacial bonding		Internal restraint by a stainless steel bar without interfacial bonding				
<i>As/Ac</i> (%)	0.8	4.9	1.1	1.1	3.3	5.8	9.1	13.1	17.8
Transverse direction									
Restraint condition	No restraint		No restraint	Stirrup	No restraint				
<i>As/Ac</i> (%)	–	–	–	0.7	–				
Method to measure/estimate expansive pressure	Estimation from mortar surface strain		Estimation from concrete surface strain		Estimation from deformation of the specimen				
Expansive pressure (MPa, longitudinal direction)	1.6	4.2	5.8	5.4	7.2–8.7	7.0–7.9	6.7–7.6	7.6–7.9	7.9–9.4

2



3

4

**Table 2 Mixture proportion of the concrete.**

Unit content (kg/m <sup>3</sup> )				
Water	Cement	Sand	Gravel	K <sub>2</sub> SO <sub>4</sub>
173	337	798	965	18.85

5

6

7

8

**Table 3 Chemical composition of the cement.**

Chemical composition (%)												
LOI	SiO <sub>2</sub>	Al <sub>2</sub> O <sub>3</sub>	Fe <sub>2</sub> O <sub>3</sub>	CaO	MgO	SO <sub>3</sub>	Na <sub>2</sub> O	K <sub>2</sub> O	TiO <sub>2</sub>	P <sub>2</sub> O <sub>5</sub>	MnO	SrO
1.15	20.16	5.05	2.52	65.00	1.35	3.04	0.26	0.36	0.31	0.65	0.07	0.05

9

10

11

12

13

**Table 4 Mineral composition of the cement by Bogue equation.**

Mineral composition (%)			
C <sub>3</sub> S	C <sub>2</sub> S	C <sub>3</sub> A	C <sub>4</sub> AF
65.1	20.16	5.05	2.52

14

15

16

17

18

**Table 5 Estimated imposed strains (positive in tension/expansion).**

19

20

21

22

23

24

25

26

27

28

29

	measurement				estimation			
	$\varepsilon_{free}$ (%)	$\varepsilon_{res}$ (%)	$\varepsilon_e$ (%)	$\sigma_{DEF}$ (MPa)	$E_c$ (GPa)	$\varepsilon_{cr}$ (%)	$\varepsilon_{imp}$ (%)	$\varepsilon_{imp}/\varepsilon_{free}$ (%)
Free	2.11	-	-	-	-	-	-	-
$\phi 9.2$	-	0.38	-0.02	-1.98	8.6	-0.05	0.45	0.21
$\phi 13$	-	0.39	-0.03	-2.44	8.7	-0.06	0.47	0.22
$\phi 17$	-	0.29	-0.03	-2.92	10.8	-0.05	0.37	0.17
$\phi 26$	-	0.27	-0.03	-2.69	10.0	-0.05	0.35	0.17

$\varepsilon_{free}$ : stress-free expansion (%),  $\sigma_{DEF}$ : expansive pressure measured by the load cell (MPa)

30

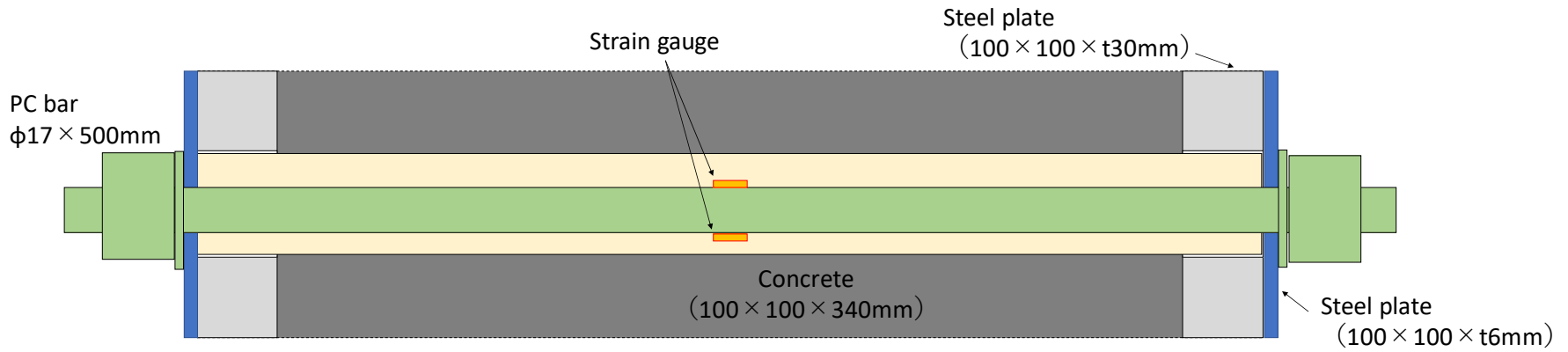
31

**Table A1 Mixture proportion of the concrete for the bi-axial restraint test.**

Unit content (kg/m <sup>3</sup> )				
Water	Cement	Sand	Gravel	K <sub>2</sub> SO <sub>4</sub>
174	290	835	973	14.5

32

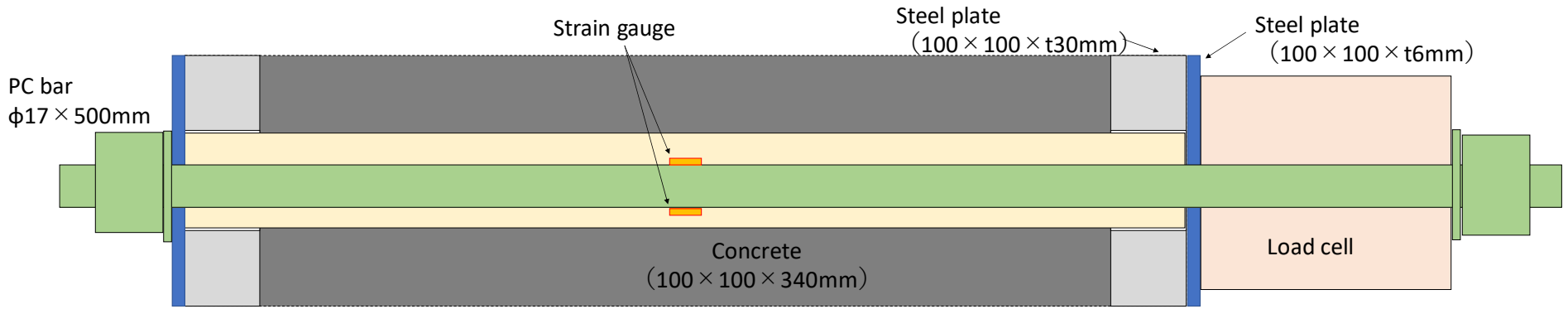
1



2

3

**(a) Specimen without a load cell**



4

5

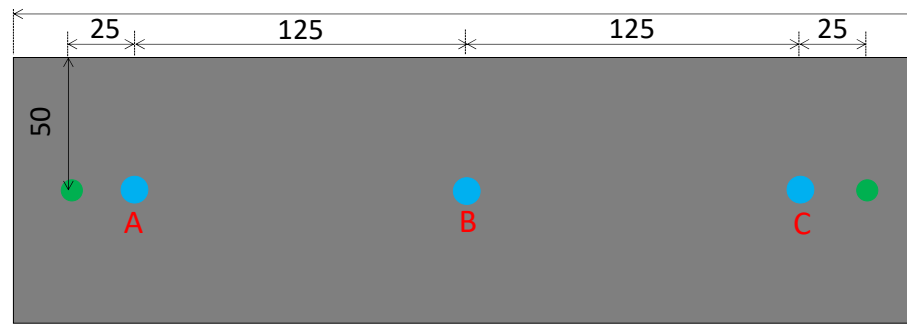
**(b) Specimen with a load cell**

6

**Figure 1 Apparatus for the expansion test.**

7

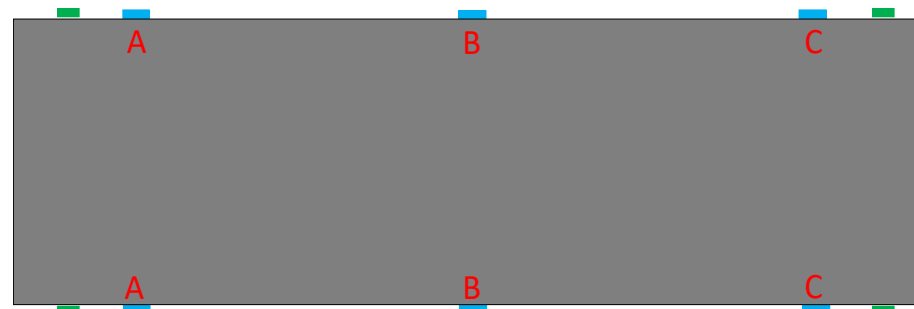
8



9

10

(a) Front view



11

12

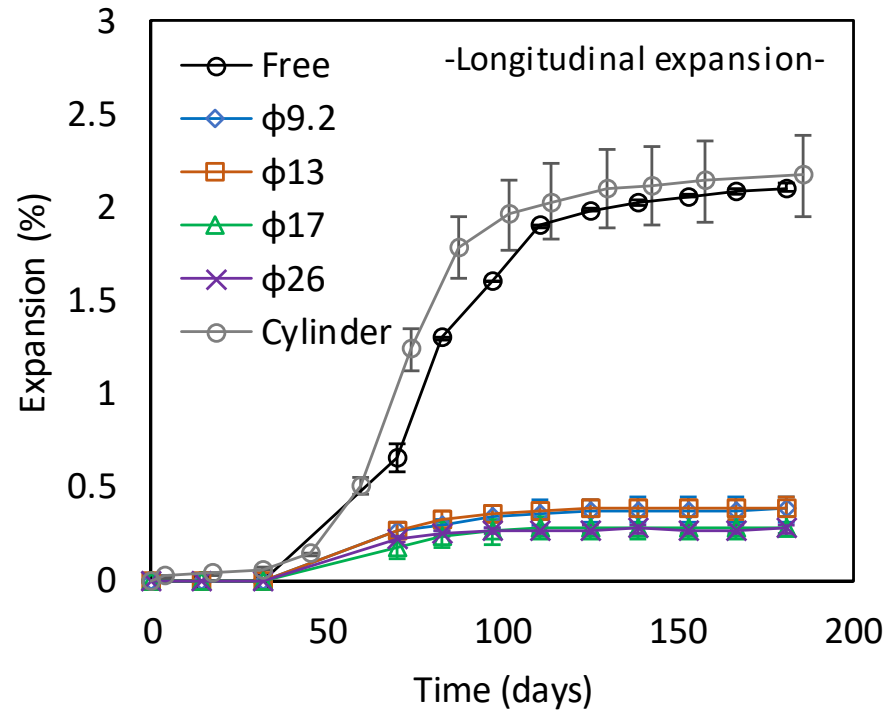
(b) Lateral view

13

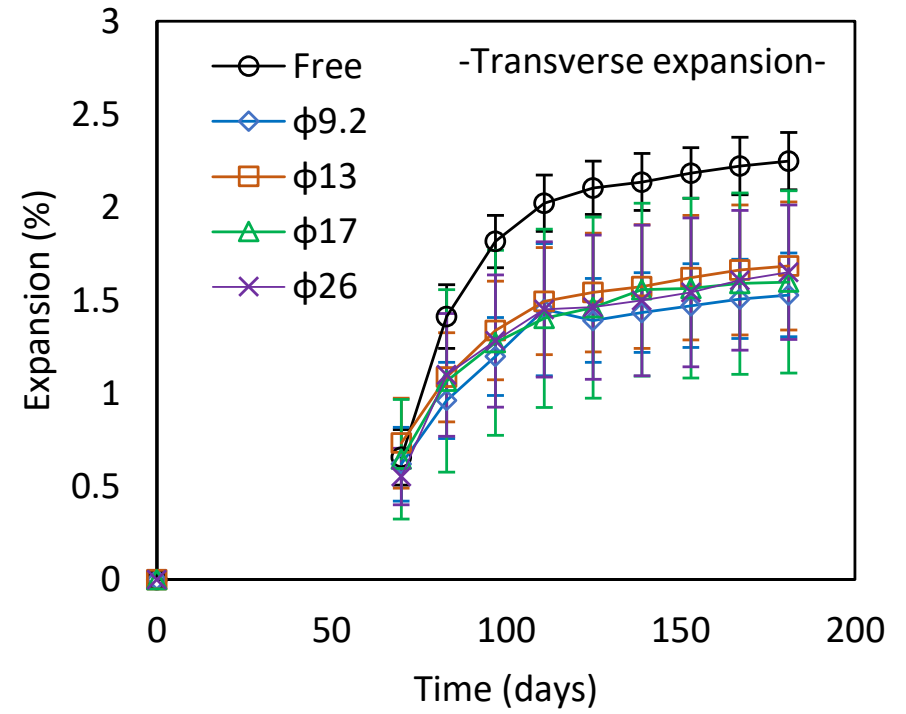
**Figure 2 Measurement points on the test specimens (green points denote the location of studs for measuring longitudinal expansion while blue points are for transversal expansion).**

14

15



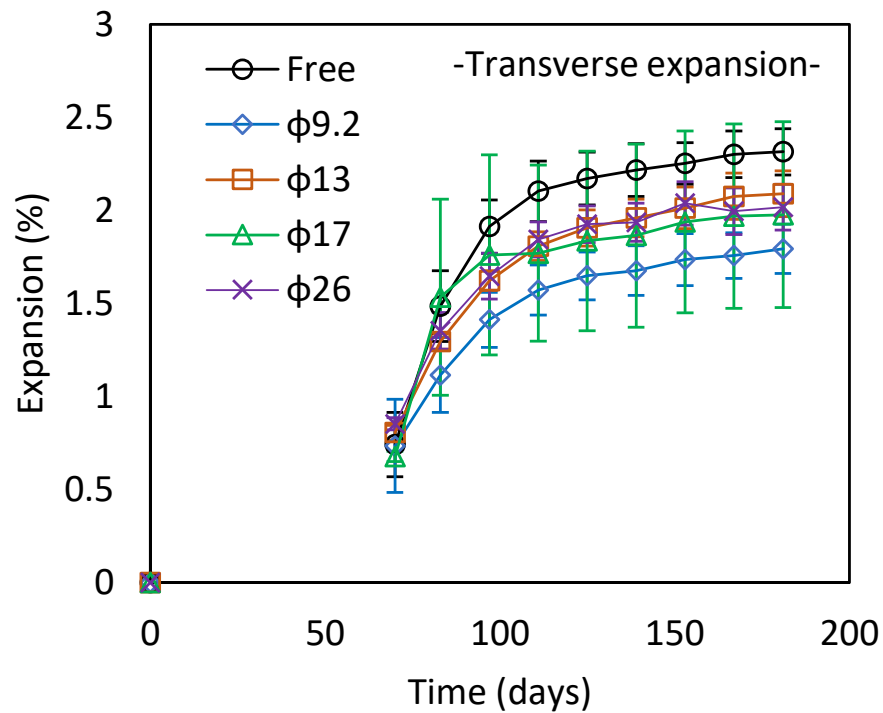
(a) Longitudinal expansion



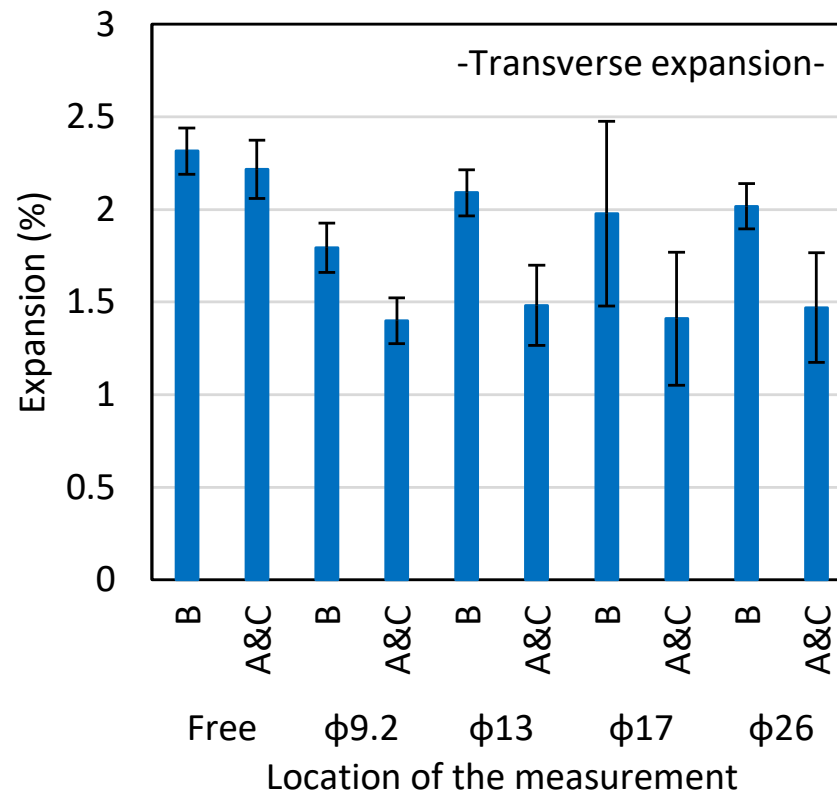
(b) Transverse expansion

Figure 3 Expansion of the concrete. Error bars indicate the standard deviation.





**(a) Transverse expansion at point B**



**(b) Transverse expansion at 181 days**

22 **Figure 4 Transverse expansion of the concrete at different locations. Point B was at the center of the longitudinal direction and A and C were**  
 23 **at 150 mm from the center. These locations are illustrated in Figure 2.**

24

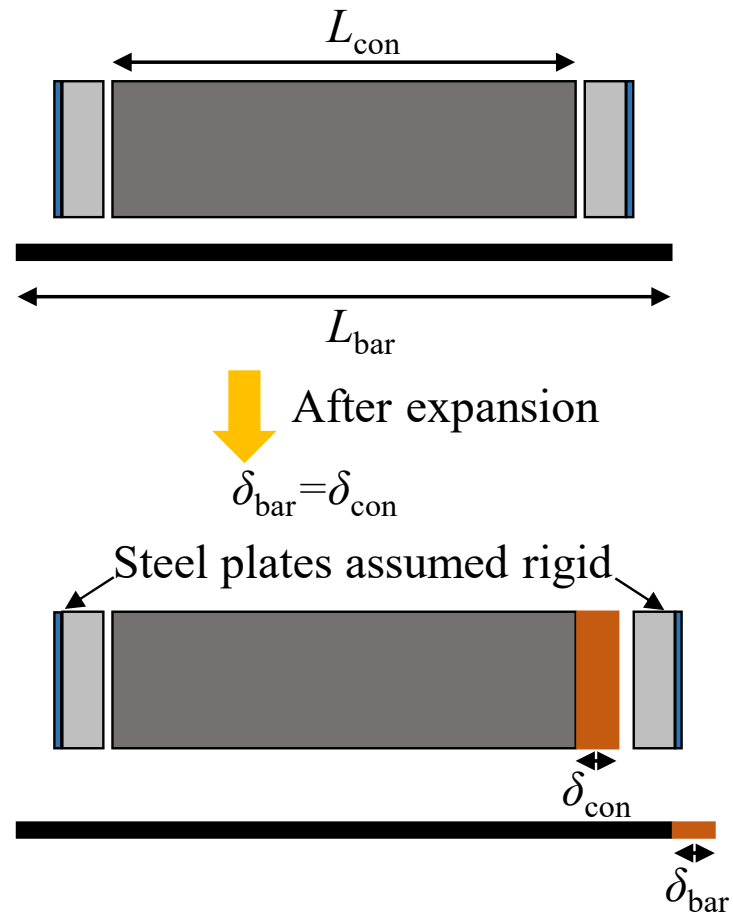
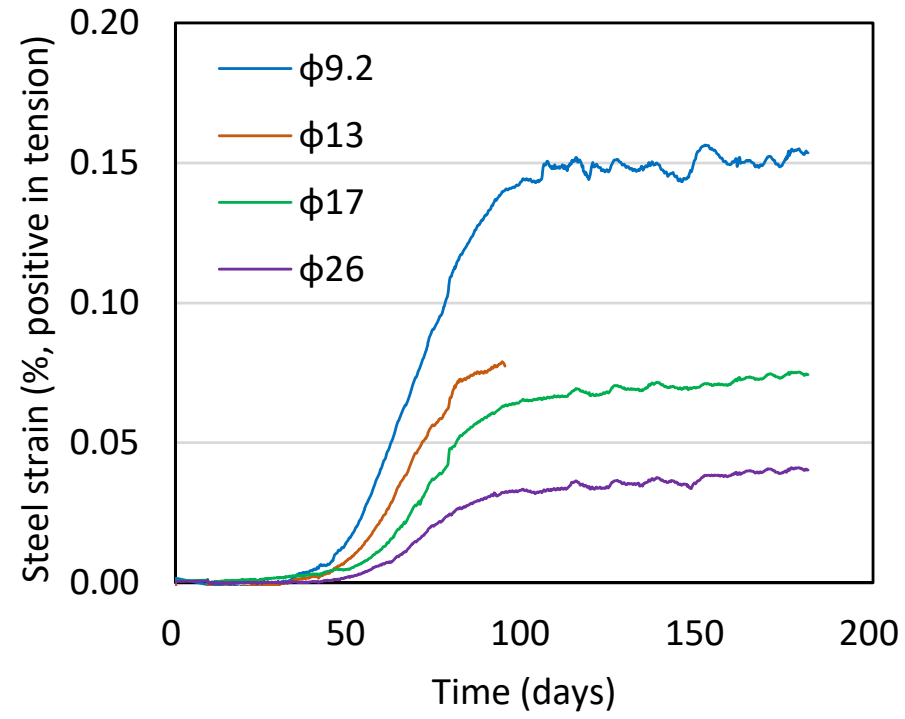


Figure 5 Schematic diagram for the calibration of the steel bar strain.

30



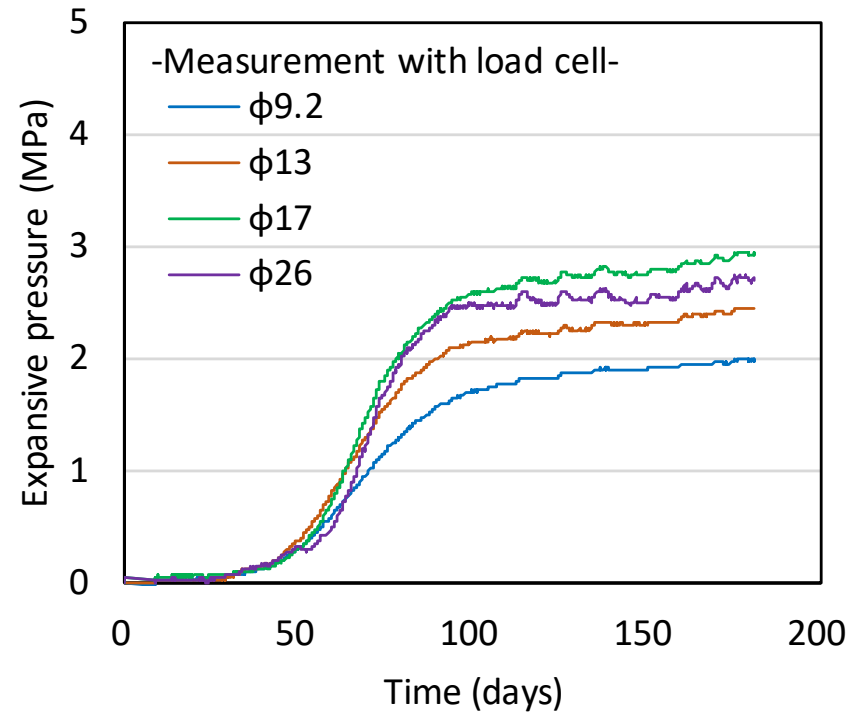
31

32

33

**Figure 6 Strain of the steel bar as measured after steel bar strain calibration.**

34



35

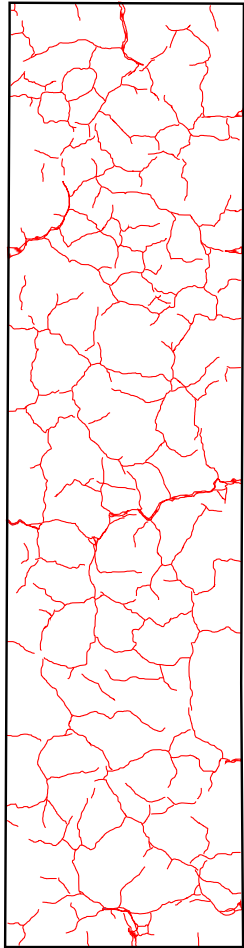
36

37

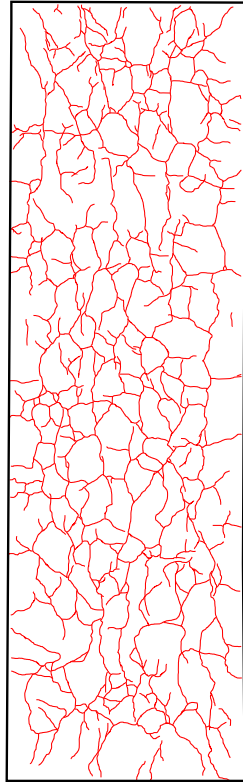
38

**Figure 7 Expansive pressure measured by the load cell (direct measurement).**

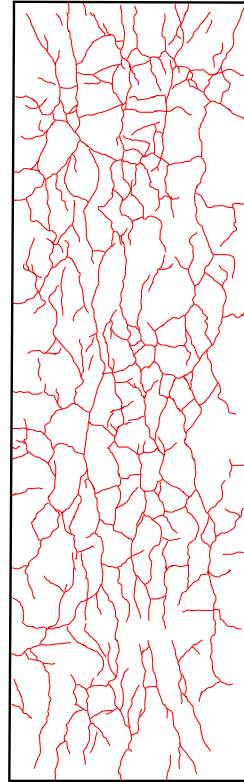




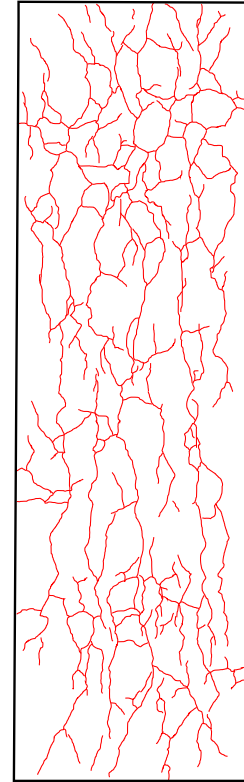
**Free expansion**



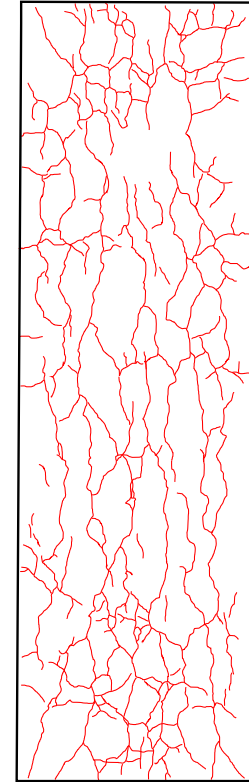
**$\Phi 9.2$**



**$\Phi 13$**

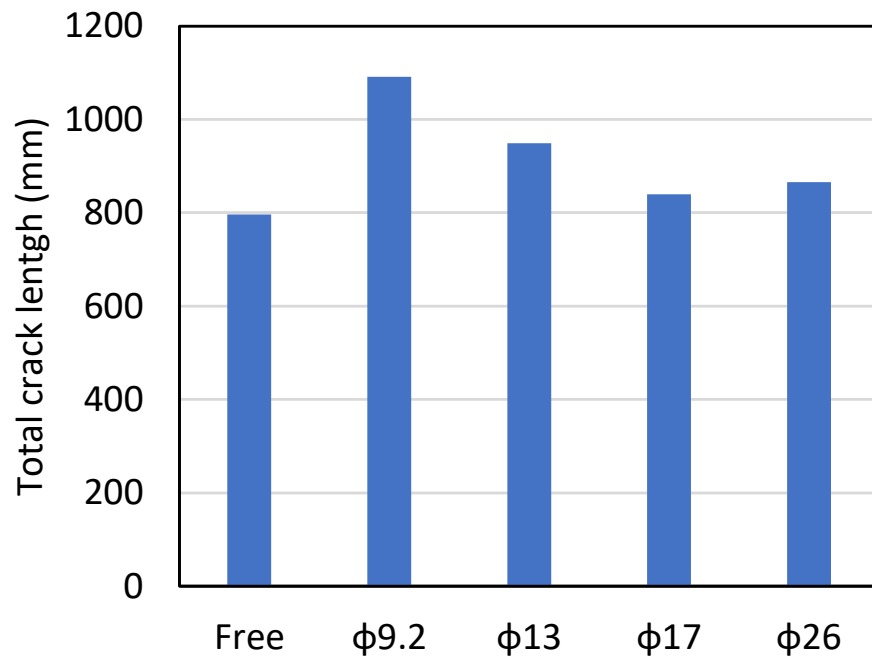


**$\Phi 17$**

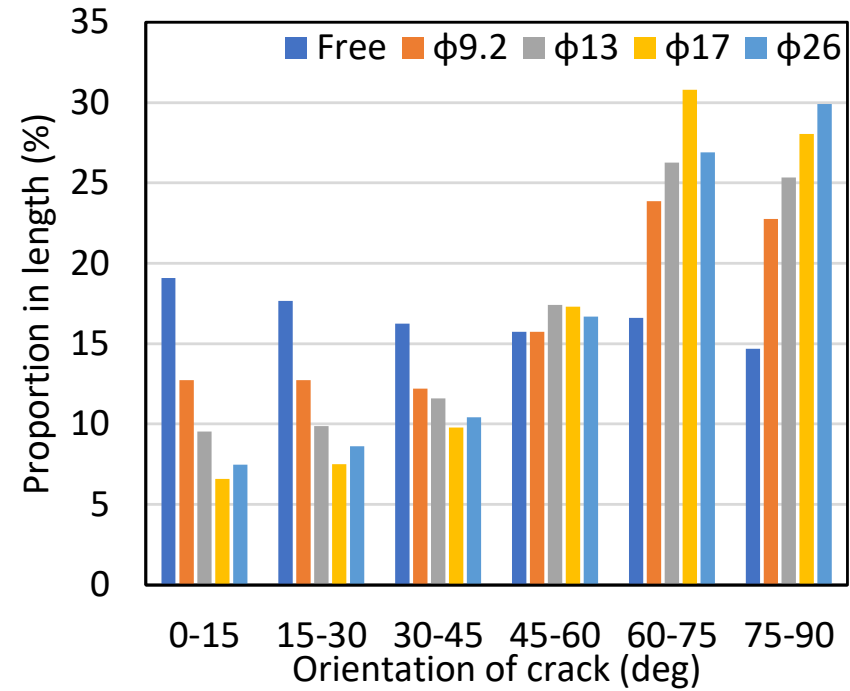


**$\Phi 26$**

39 **Figure 8 Surface crack patterns of the concrete specimens at 181 days. Note that the length of the stress-free and restrained specimens were**  
40 **400 mm and 340 mm, respectively.**  
41

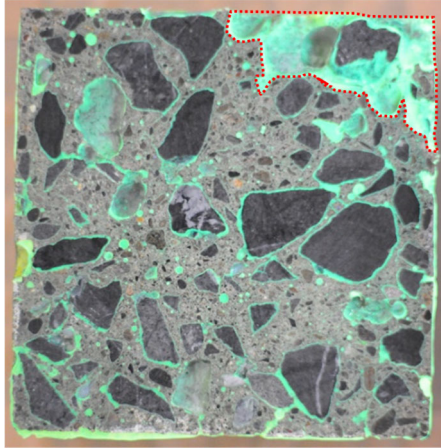


(a) Total length

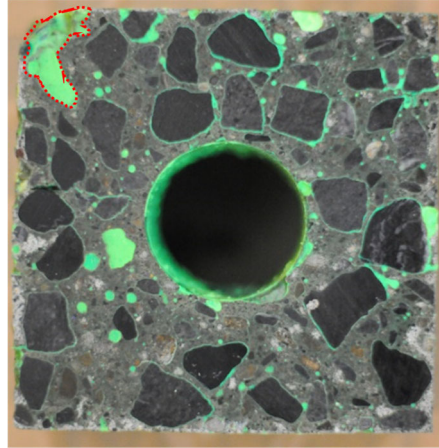


(b) Crack orientation

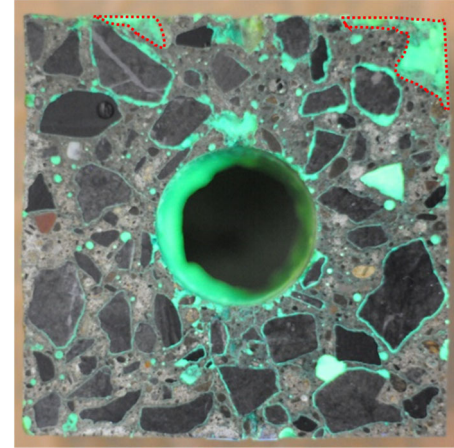
42 **Figure 9 Total length and orientation of the surface cracks. Note that the orientation of crack of 90 (deg.) corresponds to the longitudinal**  
 43 **direction whilst 0 (deg.) corresponds to the transverse direction.**



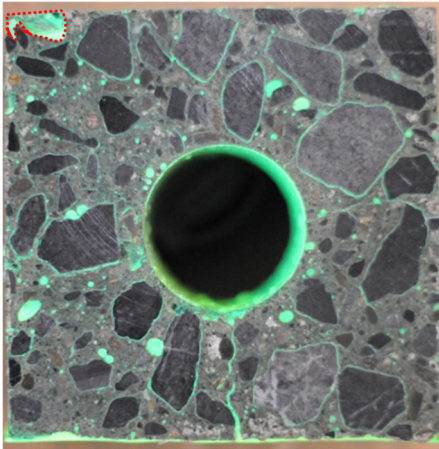
**Free expansion**



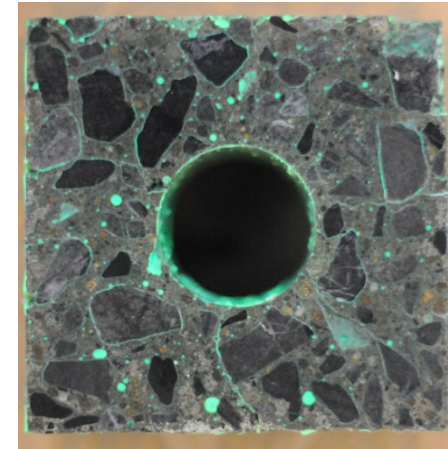
**Φ9.2**



**Φ13**



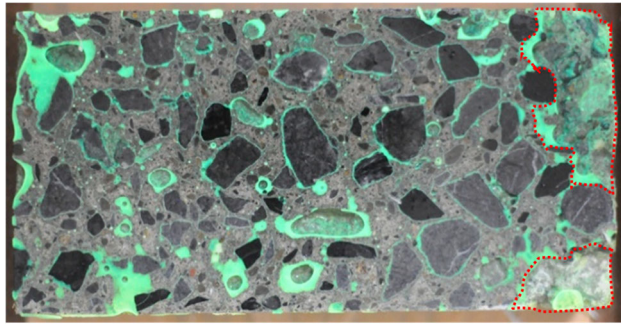
**Φ17**



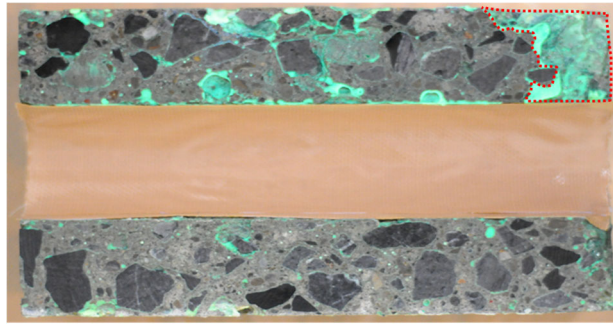
**Φ26**

**Figure 10 Internal crack pattern in the transverse direction.**

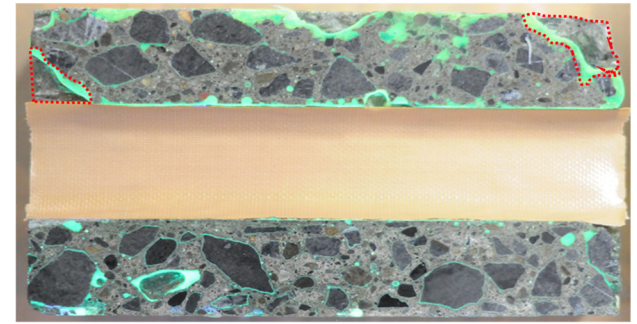




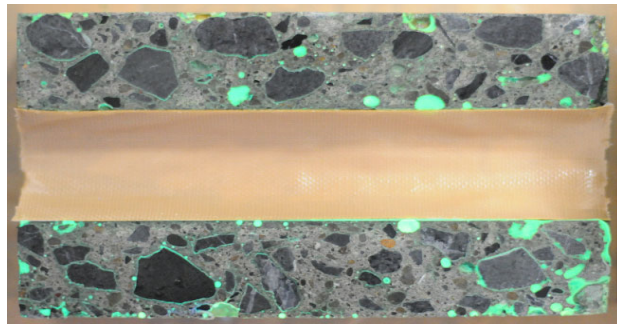
**Free expansion**



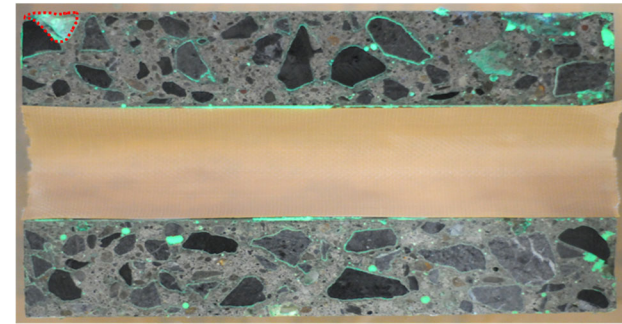
**Φ9.2**



**Φ13**



**Φ17**

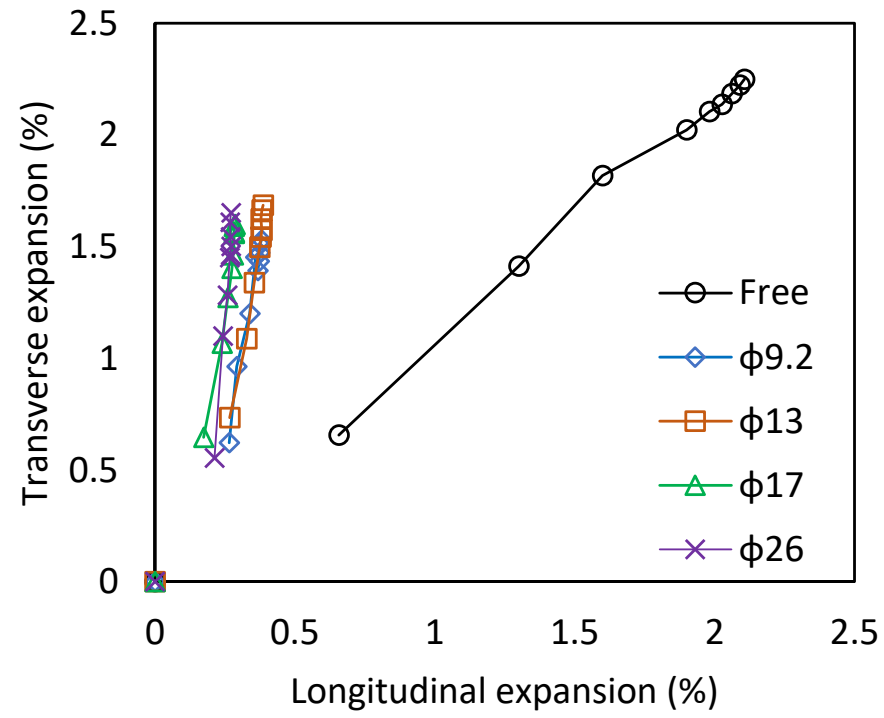


**Φ26**

**Figure 11 Internal crack pattern in the longitudinal direction.**

45  
46  
47  
48  
49

50



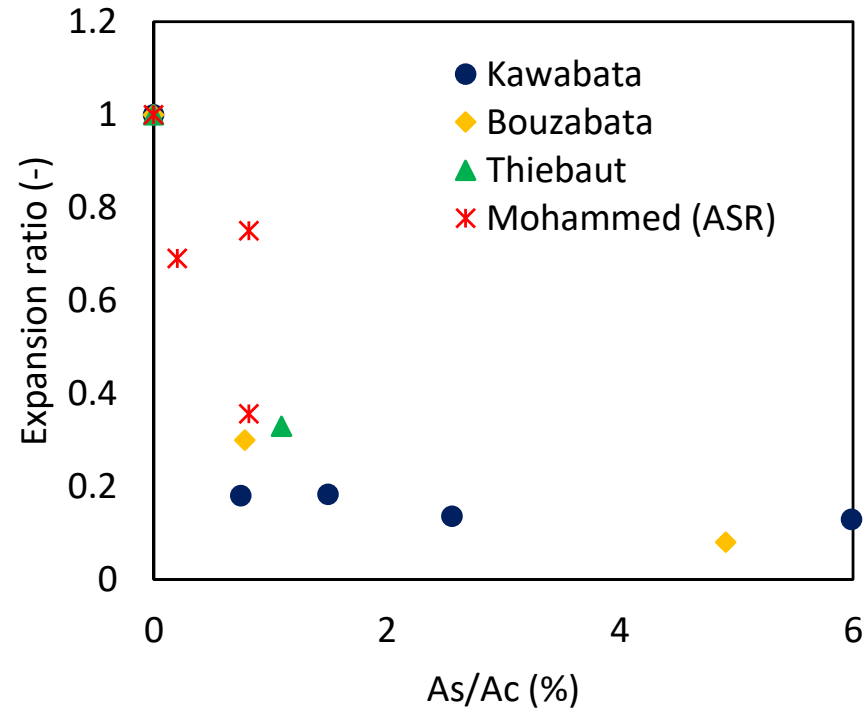
51

52

Figure 12 Longitudinal expansion vs. the transverse expansion of the concrete.

53

54



55

56

57

**Figure 13** *As/Ac* vs. the expansion ratio.

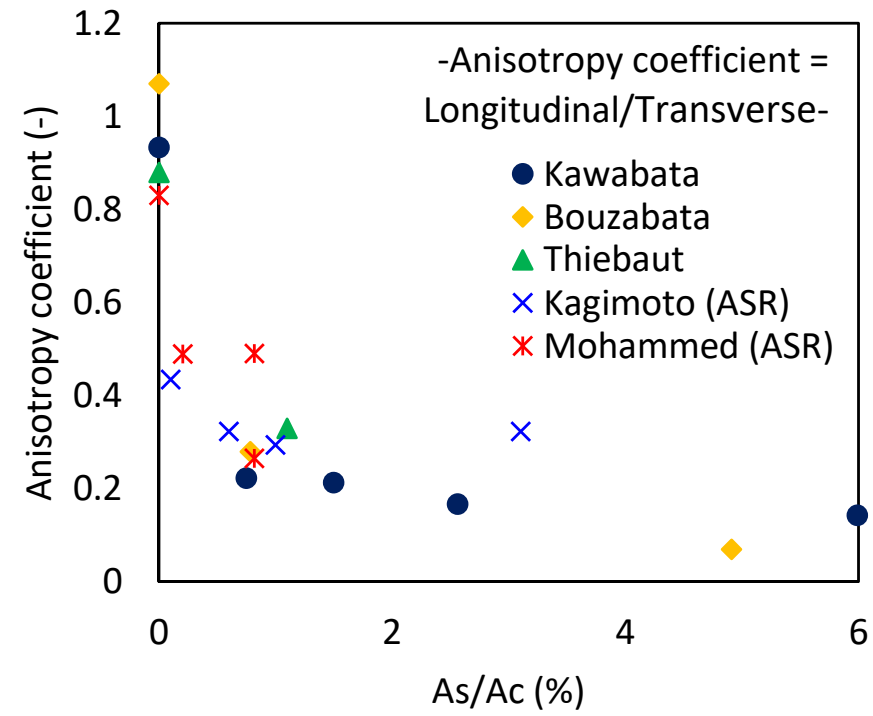
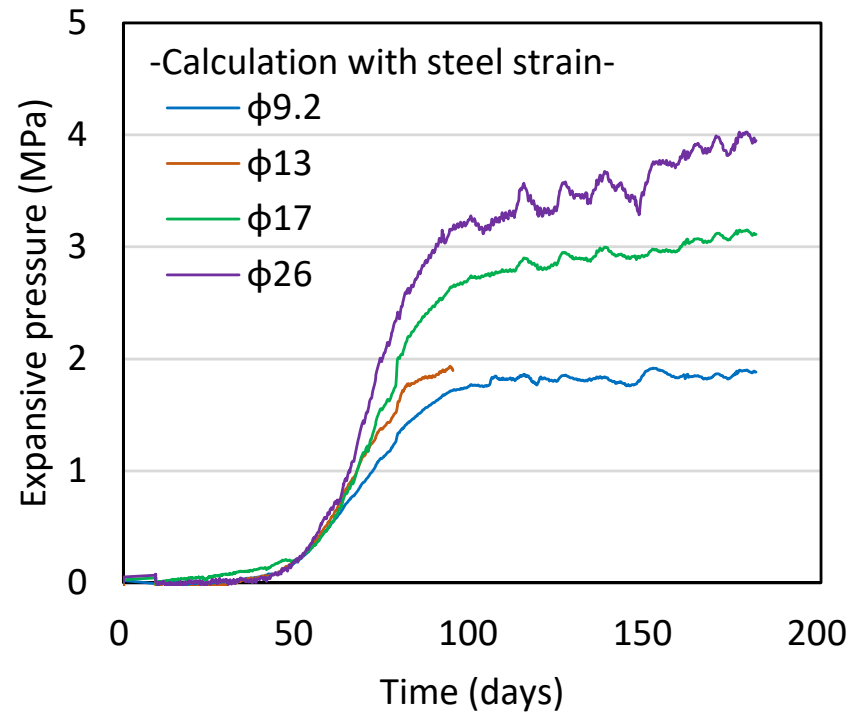


Figure 14 *As/Ac* vs. the anisotropy coefficient.

62



63

64

**Figure 15 Expansive pressure calculated using the uncalibrated steel bar strain.**

65

66

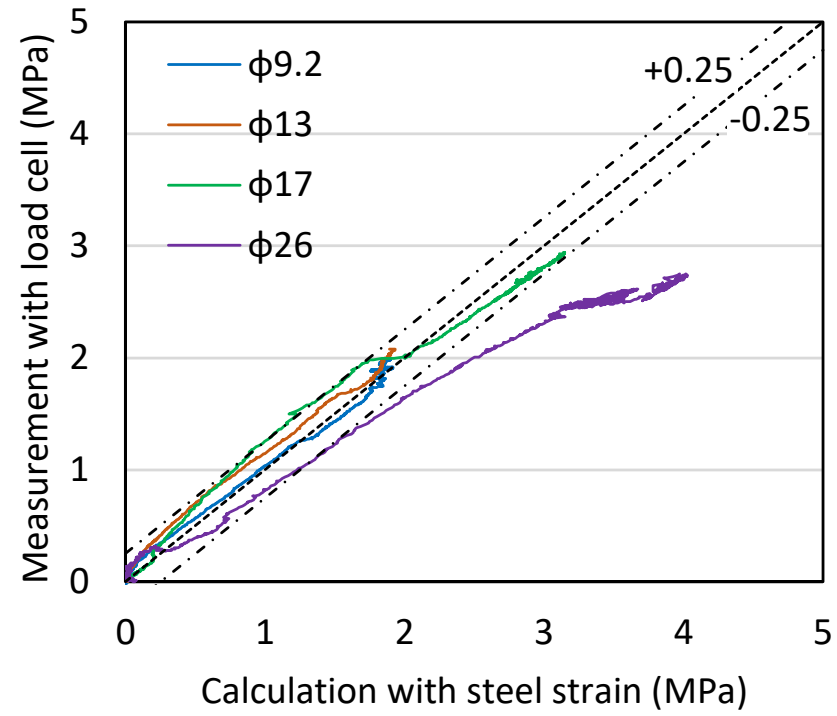
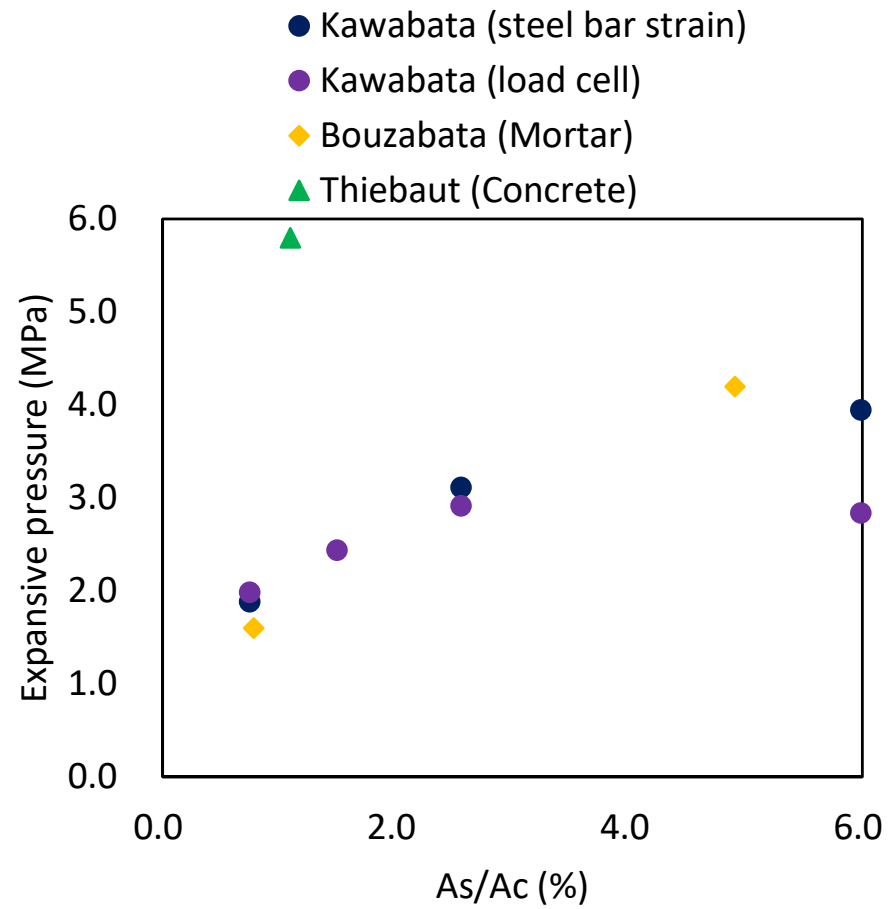


**Figure 16 Expansive pressure from the steel strain vs. the load cell measurement results.**

71



72

73

**Figure 17  $A_s/A_c$  vs. expansive pressure. The method used to calculate or measure the expansive pressure is described in parentheses.**

74

75

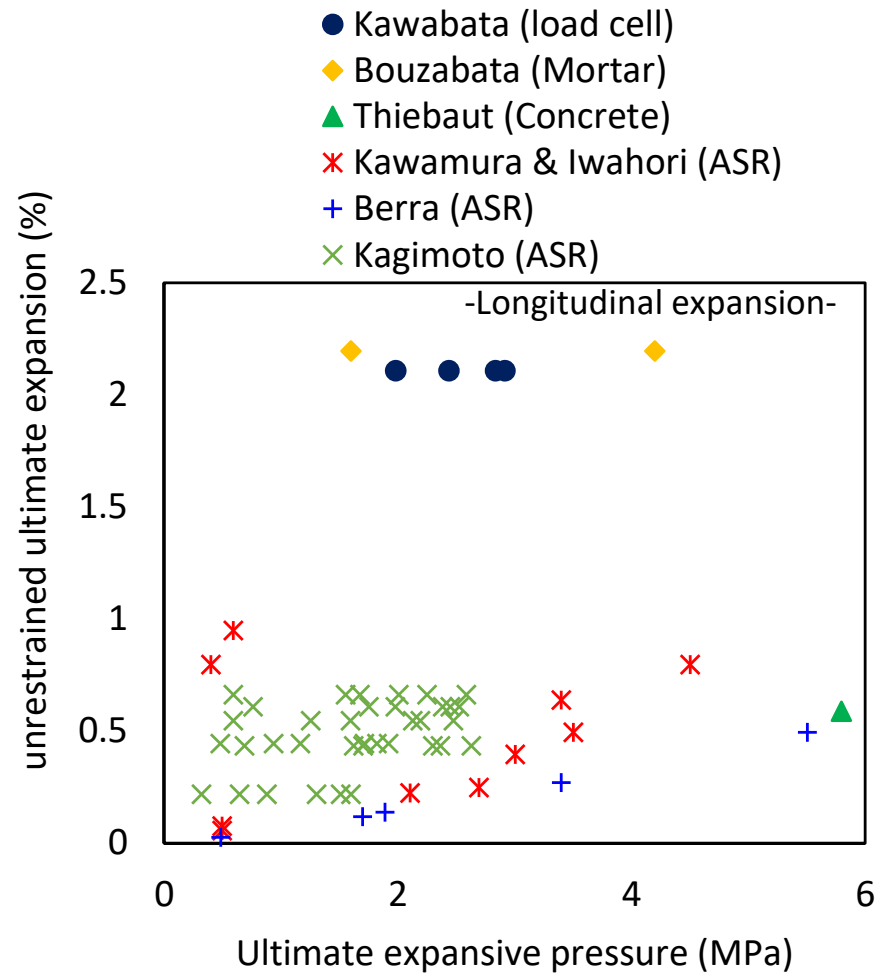
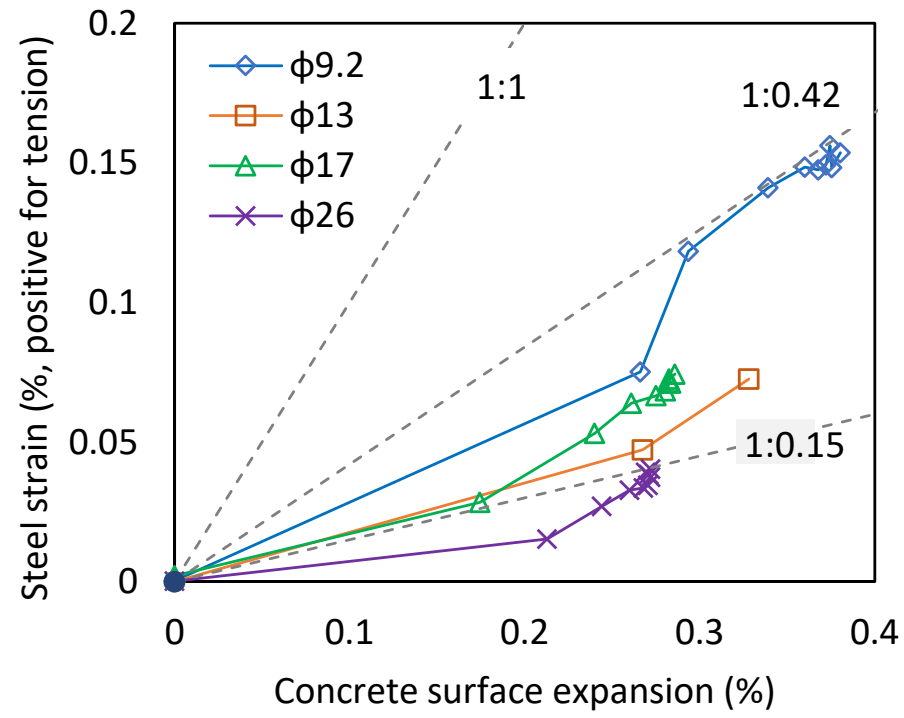


Figure 18 Ultimate expansive pressure vs. unrestrained/free ultimate expansion.



80

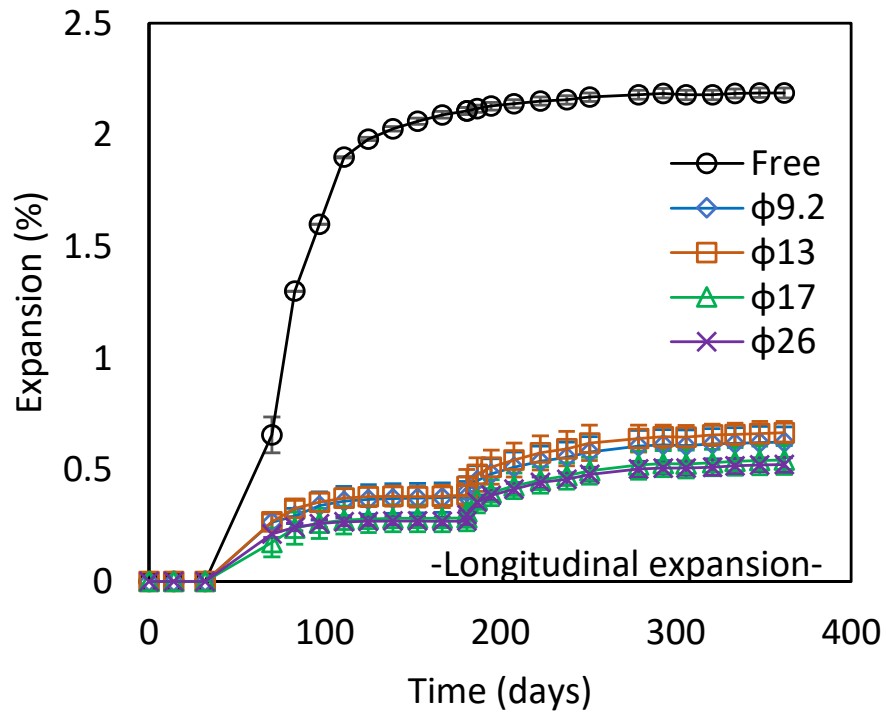


81

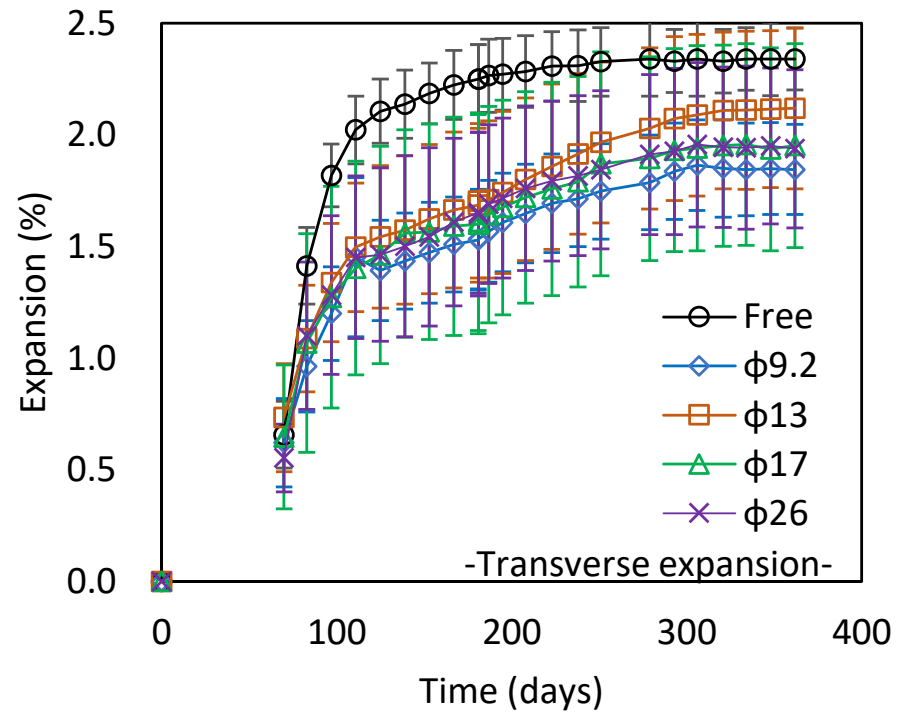
82

83

Figure 19 Concrete surface expansion vs. calibrated longitudinal steel strain.



(a) Longitudinal expansion

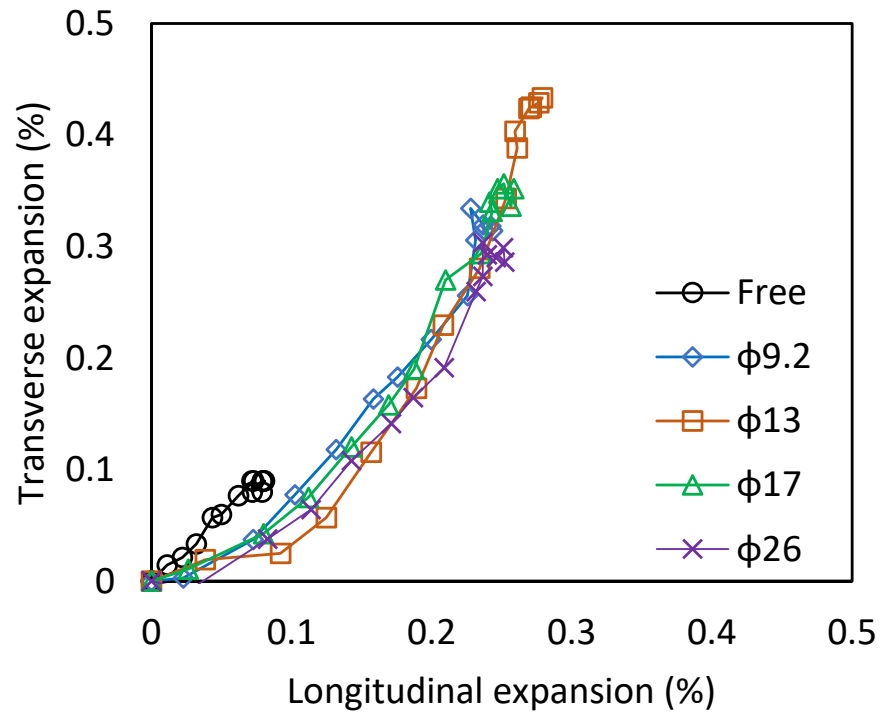


(b) Transverse expansion

Figure A1 Expansion of the concrete including releasing the restraint at 181 days.

84

85

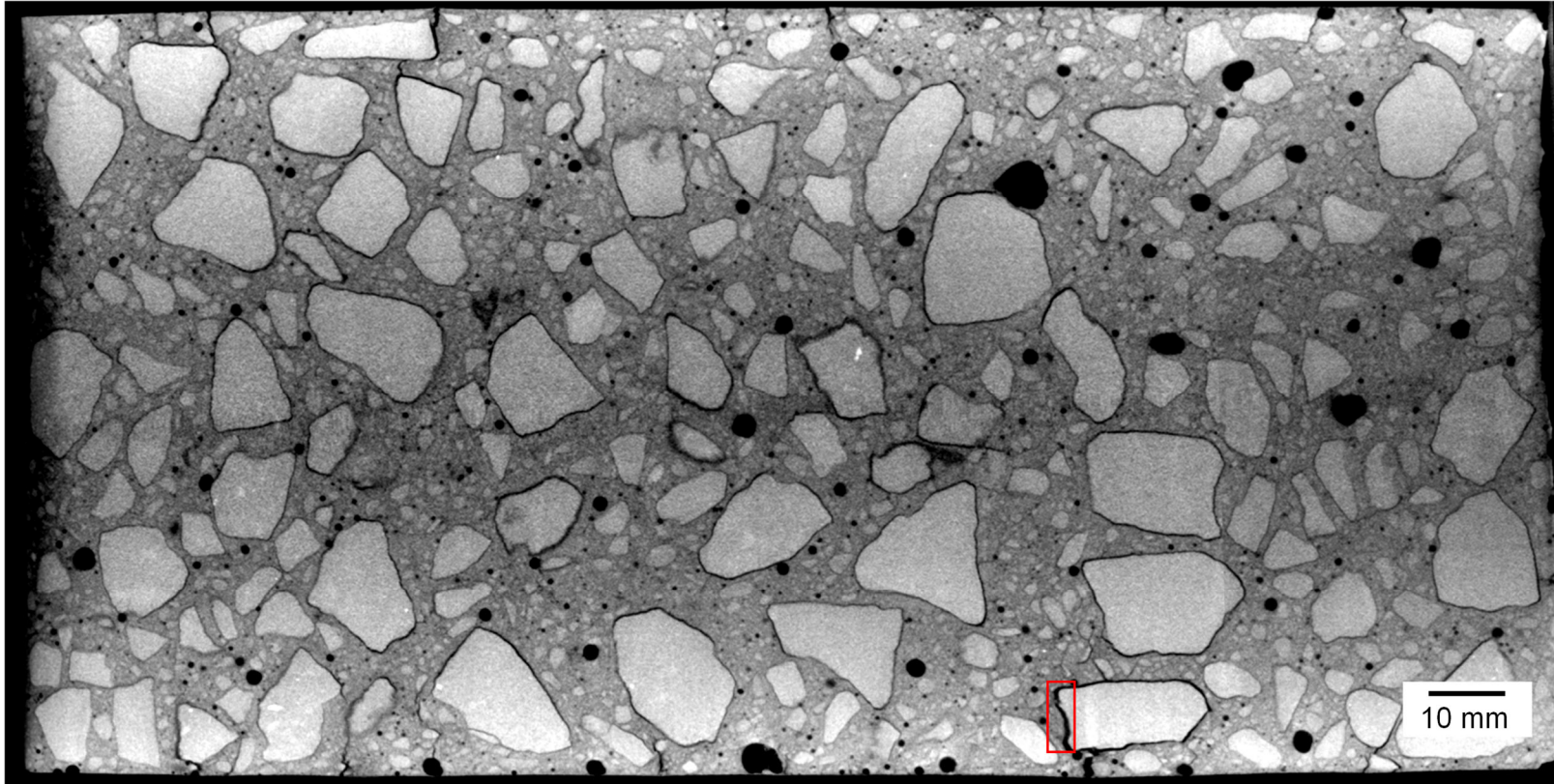


86

87 **Figure A2 Longitudinal expansion vs. transverse expansion after releasing the restraint. The expansion of the concrete after releasing the**  
 88 **restraint is normalized by subtracting the final expansion before restraint release.**

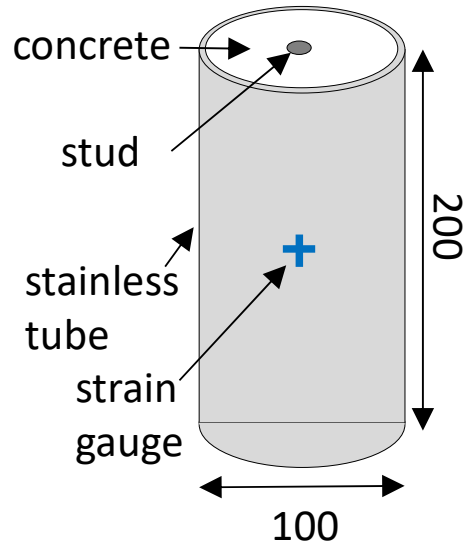
89

90



91  
92  
93

**Figure A3 X-ray CT image of the concrete cylindrical specimen. The red rectangle shows the gap with a 0.9-mm width.**



(a) Specimen details



(b) Photo

94

Figure A4 Test specimen for the bi-axial restraint.

95

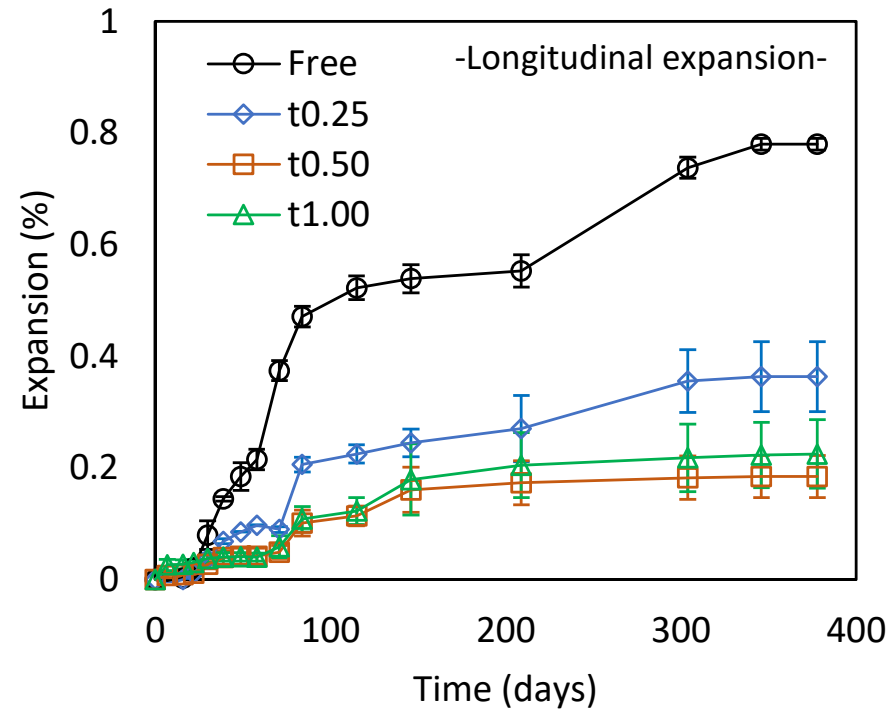
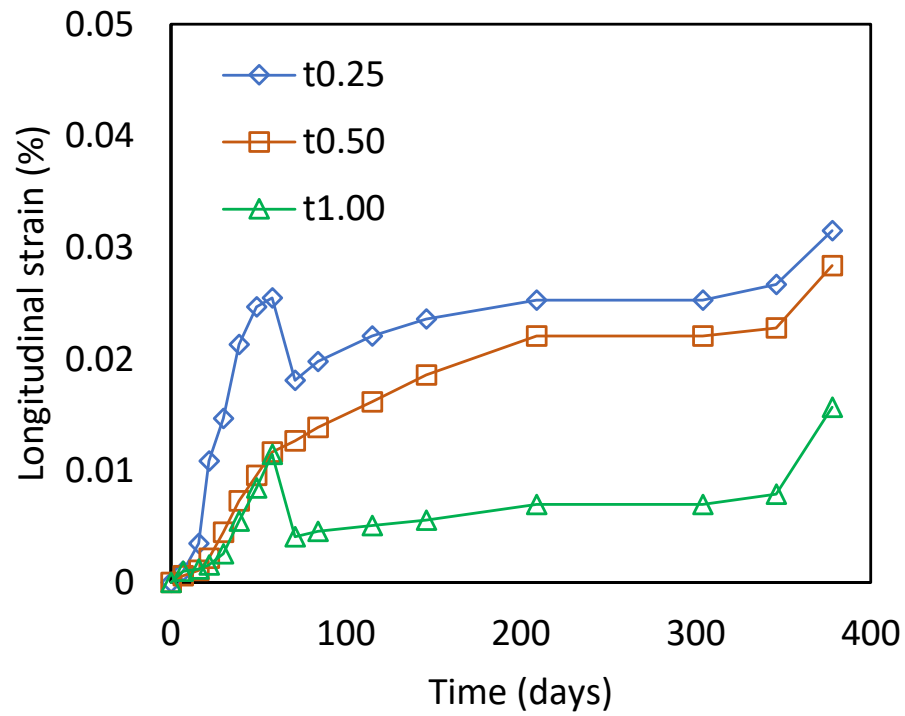
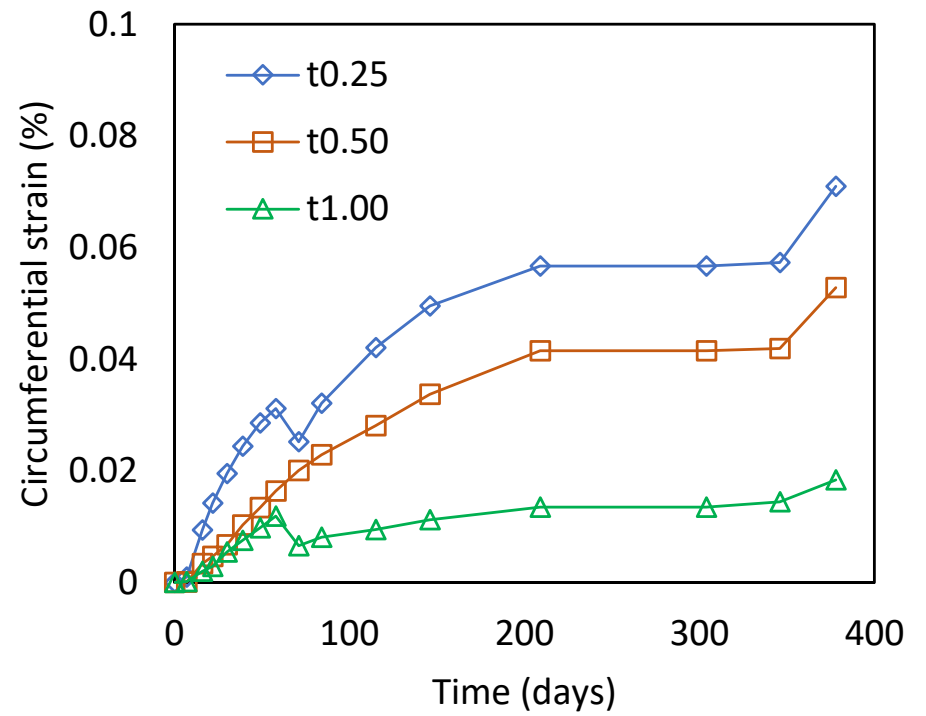


Figure A5 Longitudinal expansion of the cylindrical concrete specimen (bi-axial restraint case).



(a) Longitudinal strain

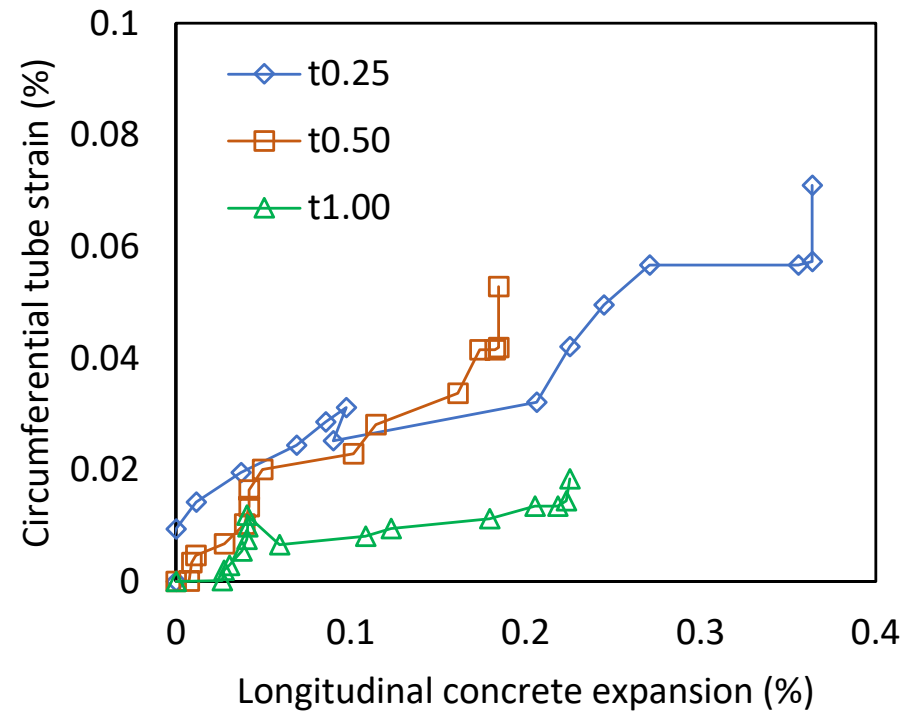


(b) Circumferential strain

Figure A6 Longitudinal and circumferential strains of the stainless tube (bi-axial restraint case).

100

101



102

103

104

**Figure A7 Longitudinal expansion of the concrete vs. circumferential strain (bi-axial restraint case).**



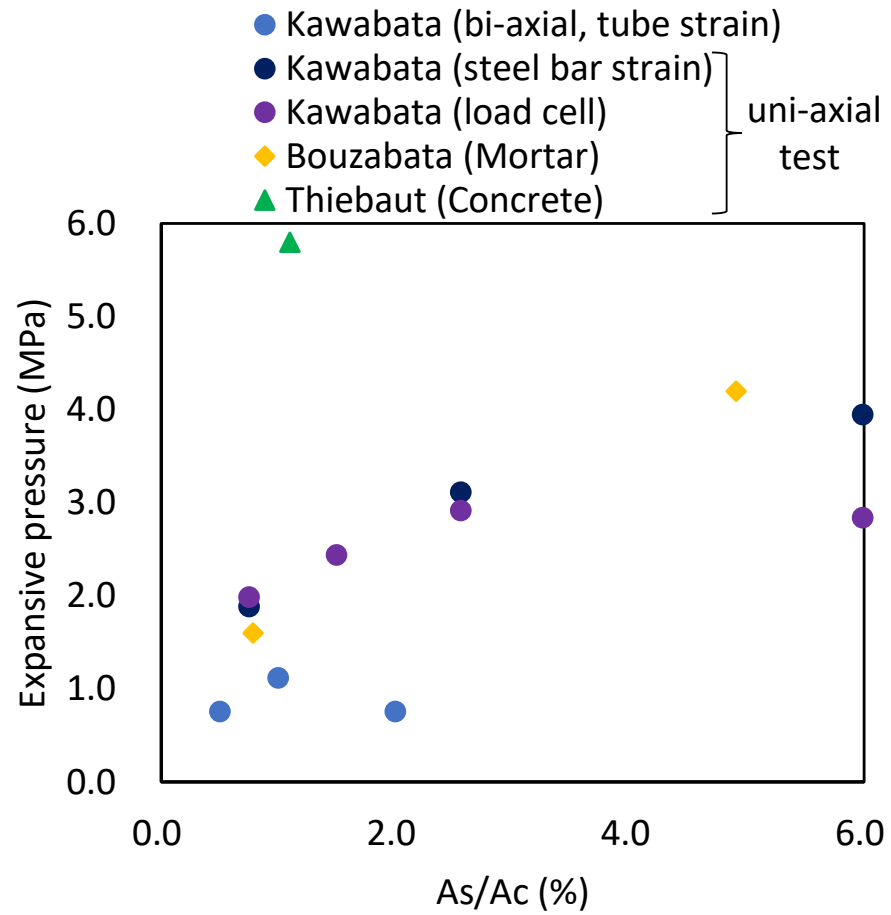


**Figure A8 *As/Ac* vs. expansive pressure.**

105

106

107